

A 20 Year Retrospective of the Advanced Noise Control Fan – Contributions to Turbofan Noise Research

Daniel L. Sutliff*
NASA Glenn Research Center
Cleveland, Ohio, 44135, USA

The Advanced Noise Control Fan (néé Active Noise Control Fan - ANCF) was utilized in the design, test, and evaluation for technical risk mitigation of most of the innovative fan noise reduction technologies developed by NASA over the past 20 years. The ANCF is a low-speed, ducted fan, testbed for measuring and understanding fan-generated aeroacoustics, duct propagation, and radiation to the farfield. It is considered a low Technology Readiness Level testbed. The international aeroacoustics research community employed the ANCF to facilitate advancement of multiple noise reduction and measurement technologies, and for code validation. From 1994 to 2016, it was located in the NASA Glenn Research Center's Aero-Acoustic Propulsion Laboratory. In 2016 the ANCF was transferred to the University of Notre Dame where it is expected to continue to positively impact ducted fan aeroacoustic research and provide STEM support. This paper summarizes the capabilities and contributions of the ANCF to the field by documenting its history. Limited data is presented, focusing on a description of the configurations, goals, and objectives of representative ANCF tests. This provides an overview of the progress of aeroacoustic research as implemented on the ANCF, as well as a background for its continued usage.

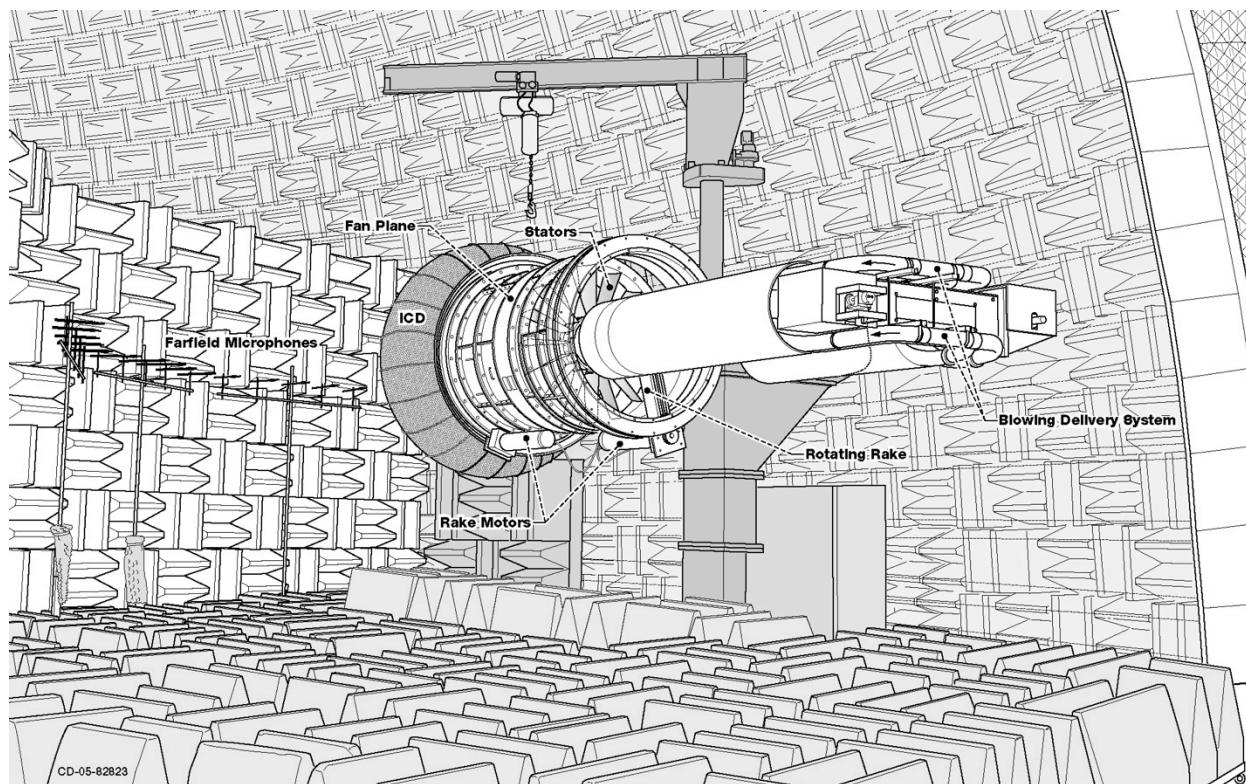


Figure A: Line Drawing of the Advanced Noise Control Fan in the Aero-Acoustic Propulsion Laboratory

* Aerospace Engineer, Acoustics Branch, AIAA Associate Member

I. Introduction

A. Rationale

The NASA Glenn Research Center has been involved in several programs¹ (Advanced Subsonic Technology, Quiet Aircraft Technology, the Fundamental Aeronautics Subsonic Fixed Wing, and currently, Advanced Aircraft Transport Technology) whose goals were the reduction of the adverse impact of aircraft noise on the public.

These programs employed multiple strategies to address the issue – code predictions (system analysis and physics-based), measurement tool development, component database acquisition – all supporting the development and application of noise reduction concepts. Several focal points, emphasis, and/or success metrics were stressed in individual programs, but consistent across all these programs, was a focus on the reduction in noise attributed to the turbofan engine.

Novel means of noise reduction were required in order to meet the continually aggressive noise reduction targets. In order to implement NASA's philosophy of high-risk / high-benefit technologies (i.e. "Fail-Smart"), a highly flexible, low cost, testbed was needed to quickly evaluate and improve proposed concepts.

B. Basics of Aircraft Noise

Aircraft noise³ can be separated into two general sources: (i) propulsion noise and (ii) airframe noise. Depending on the aircraft and flight condition, the relative levels of these sources varies; generally, the turbofan noise dominates.

Turbofan noise results from a variety of sources within the engine (Figure 1). A major component of turbofan noise is due to rotor-stator and other interactions, coupled to duct propagation, which then radiates to the farfield. This source of noise is generated by the impingement of the rotor wake on the stator. This periodic interaction generates a pressure response from the stator that coalesces into acoustic duct modes⁴. Figure 2 is a flow chart of the generation and measurement of fan noise.

Currently, the primary means to reduce propulsion noise is through careful design of the source (though acoustics takes a lower priority relative to other concerns, most notably performance, operability, reliability, and maintenance) or attenuation after the noise is generated⁵. A few examples of source design include blade count/spacing/shaping⁶. The primary method for reducing noise after it is generated is through the installation of honeycomb/resistance sheet passively absorptive liners⁷ in locations internal to the turbofan with relatively moderate aerodynamic and thermodynamic conditions (nacelle walls compared to the core, for example).

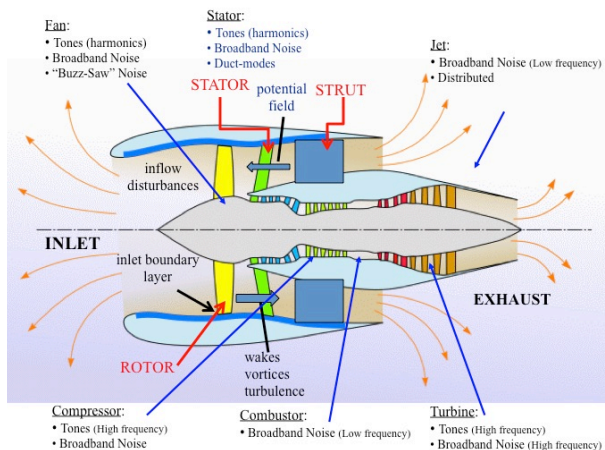


Figure 1: Sources of Turbofan Noise

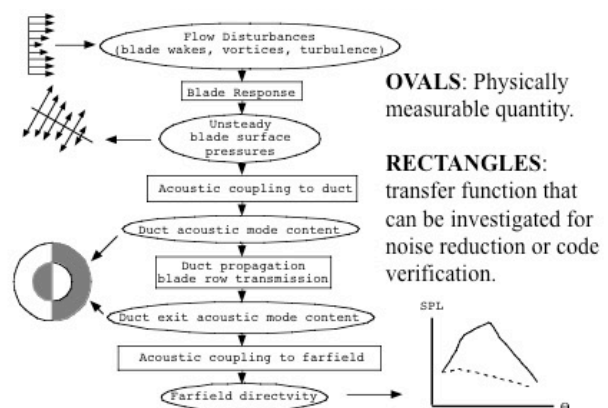


Figure 2: Rotor-Stator Interaction Schematic

II. Background

Laurence J. Heidelberg conceived the Active Noise Control Fan (original name) (ANCF) in the early 1990s as a low-cost experimental testbed for developing fan noise reduction technologies. Originally this was specifically Active Noise Control (ANC), but he also foresaw its usefulness for acoustic database enlargement to aid in the understanding of aero-acoustic physics and code validation. He also oversaw the design, installation, and early checkouts. It has been upgraded several times over the last 20 years in order to continue to make significant contributions in the aero-acoustics field, while located at the NASA Glenn Research Center.

A. Basic Features

The ANCF^{8,9,10} is a highly configurable 4-foot diameter ducted fan located in the Aero-Acoustic Propulsion Laboratory¹¹ (AAPL) at the NASA Glenn Research Center (for the period covered in this paper). The AAPL is a hemispherical anechoic (above 125 Hz) test facility used for noise measurements. An exterior view of the 65-foot high dome is shown in Figure 3. The early ANCF, shown in Figure 4, operated inside an enclosed, compact, farfield arena designed¹² such that it is in an anechoic environment (Figure 5).

The nominal operating condition¹³ of the ANCF is 1886 revolutions-per-minute-corrected (RPMc) resulting in a tip speed of 400 ft/sec, an inlet duct Mach number of ~0.15, and a fundamental blade passing frequency of ~500 Hz. The fan speed can vary from 100 to 2400 RPMc. The frequency range of 250 Hz to 2.5 kHz is representative of the range of concern for community noise impact, based on the EPNL metric. The maximum rotor tip speed of ~500 ft/sec and the duct Mach number of up to 0.16 is low, but allows for limited studies on the effect of flow. The fan pressure ratio¹⁴ is a few inches of H₂O – therefore it is not relevant to study turbofan performance utilizing the ANCF.

The ANCF can be run rotor alone, and the pitch of the 16 fan blades, nominally 28°, can be adjusted to 18° or 38°. A variable count stator hub is attached to the center-body downstream of the fan to test rotor/stator interactions. Stator counts can vary and be set at any angle. Inlet flow disturbances can be simulated using circumferentially distributed, radially extended, rods installed in front of the rotor.

An Inflow Control Device (ICD) is integrated into the ANCF inlet lip. An ICD¹⁵ is used for static engine testing to break up ground vortices and equalize the turbulence that would otherwise be ingested by the fan and create spurious noise. The ANCF ICD was an equipotential surface with longitudinal segments. The original ICD had 11-longitudinal segments. As this was eventually shown to generate cut-on modes based on the 11 segments, a 22-segment ICD was built. Fine wire mesh on either side of the honeycomb structure of the ICD was used to further reduce the turbulence.

The unique feature of the ANCF, and the sine qua non of the ANCF is the Rotating Rake¹⁶. The Rotating Rake, based on the modal theory of Tyler-Sofrin⁴, provides a complete map of the acoustic duct modes present in a ducted fan and hence enabled much of the research described in the next sections. In addition, multiple aero-acoustic measurement capabilities are integrated into the ANCF rig

The general Technology Readiness Level (TRL) of the ANCF is considered to be 2-3 for representing a turbofan engine.

B. CFANS Derivative

A Configurable Fan Artificial Noise System¹⁷ (CFANS) was developed and utilized to generate and control circumferential modes (m) and to generate radial modes (n). The system consists of 4 axially distributed rows, each with 16 circumferentially distributed sets of electromagnetic drivers flush mounted on the inner wall. There are two spool pieces, each having 2 driver rows. A LabviewTM program is used to generate the waveforms sent to each driver independently, in the proper phase relationship to generate the desired circumferential mode. The signals to each row can be adjusted to affect the radial distribution, if desired. The practical limits of the system are $|m\text{-order}| \leq 7$, and frequency ≤ 1500 Hz

C. Programmatic Impact

The ANCF was the primary component in two NASA Research Agreements, six Small Business Independent Research grants, four Space Act Agreements, two internal Glenn Strategic/Director's Research Funds, and four Aero Acoustic Research Consortium programs. These were integrated in GRC's noise reduction program milestones. It is the only complete aero-acoustic data/geometry set publicly available. Approximately 100 documents were published based on ANCF tests, data, and/or geometry (up to ~4-6 per AIAA Aero-Acoustics Conference).

Almost all of the fan noise reduction concepts and CAA prediction methods for fan tones were evaluated on, or using data from the ANCF. While the general development path for noise-reduction concept development is a sequence of increasing TRL models or tests, a few concepts have gone directly from a proof-of-concept on ANCF to a full-scale turbofan engine test. The most notable concepts were the HQ-tubes on the Honeywell TECH7000¹⁸ and the highly successful Over-the-Rotor Foam Metal Liner installed on the Williams International FJ44¹⁹. Manufacturing techniques and the efficacy of an advanced liner was validated on the ANCF prior to a recent flight test on a Boeing 737 MAX²⁰.

In addition to the direct contributions made through studies on the ANCF, the capabilities, skill set, and experience developed by the team enabled several significant contributions to the greater NASA mission. Perhaps the most notable was the participation in the NESC Return-to-Flight Flow-liner Cracking root-cause determination²¹. Also, the unique UCFANS series of tests that contributed to the ERA Hybrid Wing Body shielding studies²² were based on ANCF/CFANS lessons learned.

The remainder of this paper provides brief summaries of a number of studies conducted using the ANCF. The reader is directed to the supporting references for more thorough discussions of the individual topics.



Figure 3: The ANCF is Located in the AAPL



Figure 4: The ANCF Early Days

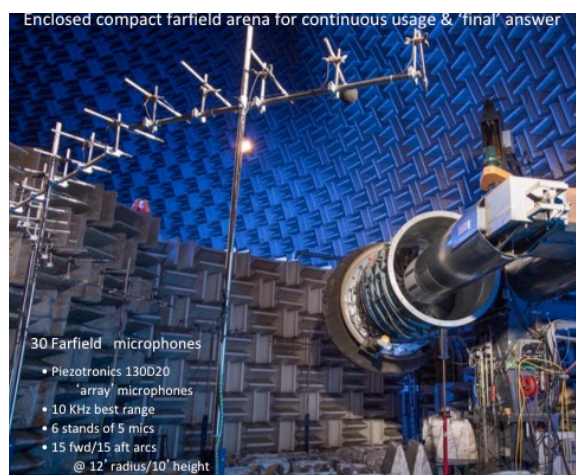


Figure 5: The ANCF in the Compact Farfield Arena

III. Historical Studies

The Active Noise Control Fan's raison d'etre was to initiate and support the NASA effort in the Active Noise Control research in the 1990s. As the NASA ARMD focus changed, the 1st letter in ANCF was changed from Active to Advanced and significant research into other noise reduction concepts and aero-acoustic investigations were accomplished. Along the way, many interesting changes and events occurred. Table I presents a time line of the research emphasis over the last two decades. This section will roughly be divided between those topics, preceded by a general history.

1995	2000	2005	2010	2015
Active Noise Control		Unique Fan Noise Reduction Techniques		Novel Liner develop
Database Development / Code Validation			Array development / Rotating Rake enhancement	

Table I: Timeline of ANCF Research Emphasis

A. General

The initial checkouts of the ANCF were in May of 1994. The checkouts were primarily performed with rods mounted in the inlet. (During the period of study, inlet-guide vanes were not a feature in contemporary aircraft turbofan engine design.) The primary reason for utilizing inlet rods in the inlet was to generate extremely clear and convincing duct modal structure and strong fan tone harmonics in the farfield relative to the broadband. The database for the stator vanes was first acquired in February 1995. Initially, a long spinner (from rotor to inlet plane) was installed for evaluation of the acoustic character but dynamic issues resulted in a short spinner being used for the remainder of the history.

While the rig was located in the APPL facility, early control was from the 2nd floor of B90 (the 10x10 Wind Tunnel control room). Rotating Rake and other in-duct data were acquired with the ANCF near the wall just inside the main door opening of the AAPL. Farfield data were acquired with the ANCF located in the center of the AAPL arena. Farfield data were acquired using the AAPL sideline array. (This array consisted of 30 microphones mounted on 10' high poles, at a 40' foot radius centered on NATR).

In 2001 a "Compact Farfield Arena" to acquire farfield data was designed and installed to allow for year-round farfield acoustic testing. Two walls with anechoic wedges were placed and angled about the ANCF as it was situated in the "in-duct data" only location. The wall in front of the ANCF was fixed; the wall on the left side, where a microphone array was situated, could pivot to allow access under the mezzanine. These walls, combined with the sidewall of the AAPL, provided three anechoic surfaces for this location. The fourth 'anechoic surface' was the open main door, and of course the hemi-spherical ceiling – the floor would be covered with movable wedges to complete the anechoic environment. The microphone array arcs were at 10' to 15' horizontally from the centerline of the duct (eventually sited at 12') and level with the duct centerline in the vertical direction. Farfield data comparisons²³ between these arcs and the 40' arc showed the data was essentially similar (some increase in the low frequency broadband levels below one-half of the blade passing frequency ($\frac{1}{2}$ BPF) were noted – probably due to increased turbulence from the proximity of the wedge wall to the inlet of the ANCF of which the ICD could not fully dissipate).

A 75 horsepower (HP) motor originally powered the ANCF. Research requirements continued to increase, and in 1999 a 125 HP motor was installed to accommodate the higher fan speeds (2500 RPM) required to achieve greater modal density. The RPM increase was accomplished by reducing the rotor pitch angle to keep the torque below the design limit. The original set of fan blades was an industrial set from Crowley. These plastic blades were designed and manufactured for ventilating fans and as such were intended for flexibility of application (one blade design for any diameter/pitch) rather than aerodynamic efficiency. They were attached to a fan hub and installed in a 14.75" (hub-to-tip ratio, σ , of 0.307) center-body. A redesign of the rotor blades to create a more realistic loading and efficiency profile in preparation for the blowing rotor study was performed using rotor-design codes in 2000. The more efficient fan design resulted in increased loading which required a new 200 HP motor installation. Also, at this time the center body diameter was increased to 18" ($\sigma = 0.375$).

B. Database Development

The primary aero-acoustic database acquired from the ANCF was the variation of stator vane count and spacing. The nominal counts were (13,14,15,26,28,30) at 0.5, 1.0, and 2.0 chord spacings. The lower counts generate a cut-on BPF, while the higher vane counts result in a cut-off BPF, a design condition that is common in modern turbofans. Rotating Rake modal data and farfield spectral data exist for most of the combinations of those physical parameters^{9,10}. Figure 6 illustrates the measurement locations corresponding to the steps in the flow chart of Figure 2 and further description in this section.

The viscous wake is the 1st step in the flow chart (Figure 2) in the generation of rotor-stator interaction noise. The upwash on the stator vane from the cyclic and repetitive change in velocity and angle is the physical cause of the stator vane surface pressure fluctuations. To acquire this database, two-component hot-film data were acquired. This set-up is shown on Figure 7a. Stator vane surface unsteady pressures are the next step of the chain in the physical generation of fan noise (Figure 7b). A database of pressure and suction side pressures were acquired. Phasing is very important in the coupling of the surface pressures to duct-modes as analytically described by the Green's function radiation and is therefore retained in the processing of this data.

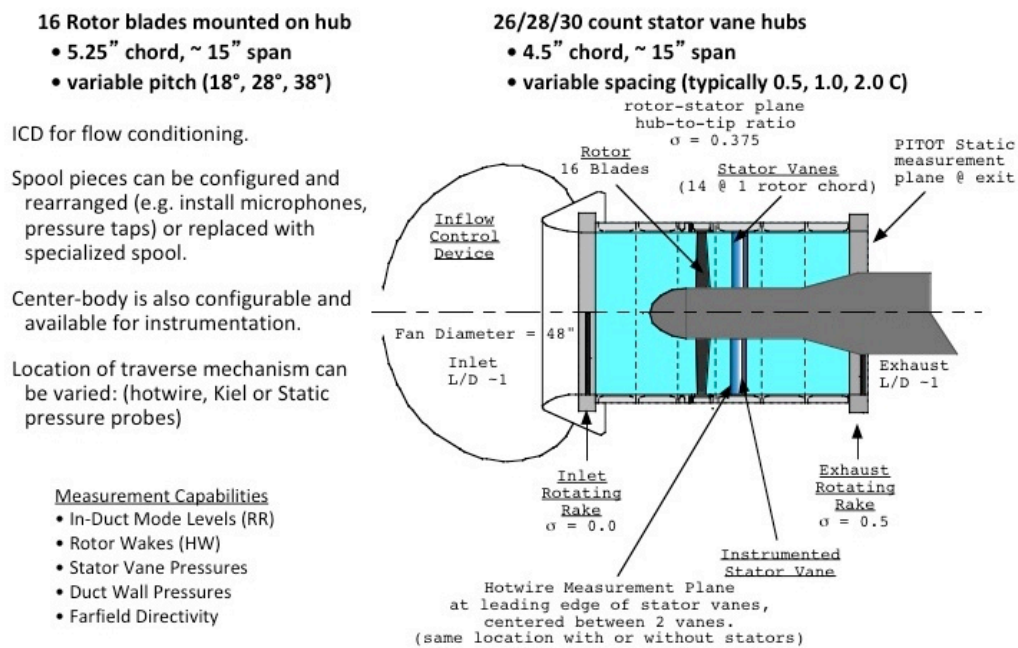


Figure 6: Schematic of ANCF Measurement Locations

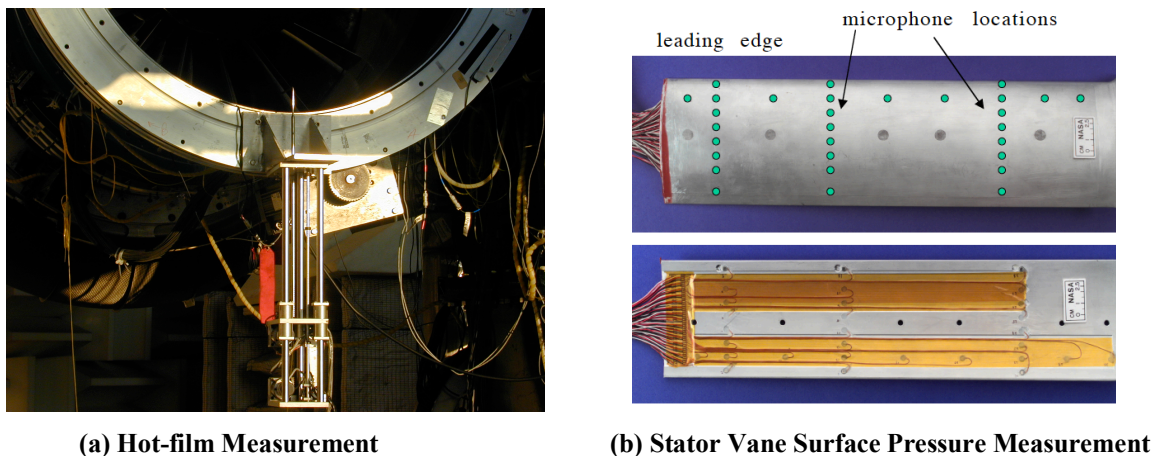


Figure 7: Aerodynamic Measurements

C. Code Verification

As a result of the ANCF's geometric flexibility and its ability to acquire multiple aero-acoustic measurements it is well suited for providing a range of conditions for code validation.

The V072²⁴ Rotor Wake/Stator Interaction Code is widely used as a simple prediction code for rotor-stator interaction. It has been used in a number of cases as a preliminary design tool. An ANCF experiment^{25,26} validated the code by comparing experimentally measured mode levels to those predicted by V072. V072 predicted mode levels based on the actual wake profiles of the ANCF rotor as measured by a 2-component hotwire. The experiment indicated that V072 reasonably predicts the mode level trends within the design limits of the code.

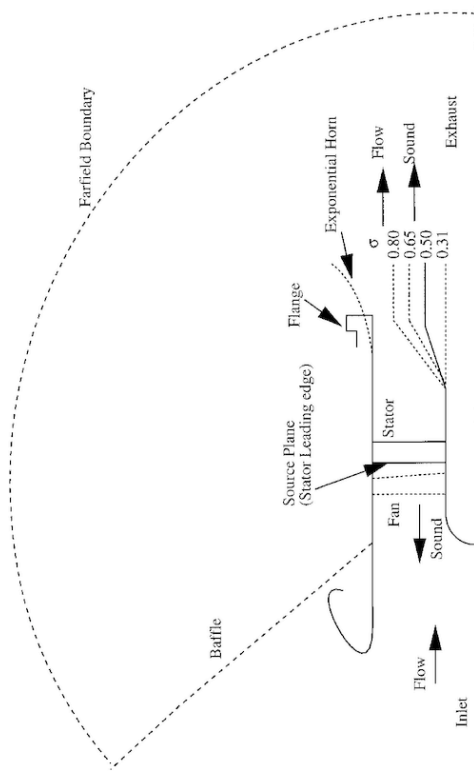
The Eversman Radiation code²⁷ is a finite-element based propagation code to predict the radiated far field directivity from in-duct modal sources. Acoustic propagation in exhaust ducts of varying cross section was examined²⁸ in a specific test. Eversman code and Rotating Rake modal measurements were employed to measure the effect of variation in the hub-to-tip ratio of the exhaust duct. Modifications to the ANCF exhaust duct inner flow path were made to increase the hub-to-tip ratio of the exhaust duct from its nominal 0.50 up to 0.80 illustrated in Figure 8a. The computed axial variations of acoustic power and phase angle of acoustic pressure from the finite element solution showed good agreement with the experimental data.

The directivity of fan tone noise is generally measured and plotted in the sideline plane and is assumed that this curve is the same for all azimuthal angles. When two or more circumferential (m-order) modes of the same tone are present in the fan duct, an interference pattern develops in the azimuthal direction in the farfield. In an investigation²⁹ two circumferential modes of similar power were generated using the ANCF. Farfield measurements showed substantial variations in the azimuthal direction. Although these configurations may have represented a worst-case scenario, the investigation implied that the validity of the current practice of assuming axis-symmetry should be questioned.

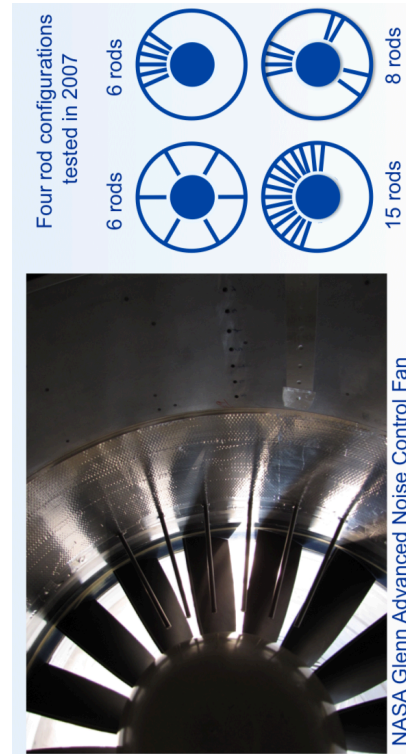
Fan inflow distortion tone noise was studied experimentally and analytically. The tone noise generated when a fan ingests circumferentially distorted flow was studied by experiments^{30,31,32,33} conducted on the ANCF. The inflow was distorted by inserting cylindrical rods radially into the duct which were arranged in circumferentially irregular patterns, installed one rotor chord length axially upstream of the fan, as shown in Figure 8b. Acoustic mode levels were measured in the inlet and exhaust duct of the fan using the Rotating Rake. Circumferential mode sound power levels were calculated from the measured data using several different methodologies described in the references.

Acoustic transmission loss (Figure 8c) test objective was to obtain the effect of geometrical obstructions on mode propagation³⁴, i.e. blockage (or transmission loss). Blockage effects were measured separately for stationary geometries (stator vanes) or for rotating geometries (fan blades). In order to provide a larger database, and taking advantage of the flexibility inherent in a no-flow condition, the existing ANCF stator vanes were pitched at a range of angles. The center-body was retained, creating a transition from $\sigma=0$ at the inlet to $\sigma=0.5$ at the exhaust exit plane. The CFANS system was used to generate modes for the study. The Rotating Rake and data acquisition system were synchronized to the CFANS rather than the fan – so the modes measured were those generated by the CFANS. That process filtered out the fan modes. The baseline case was a clean duct, with no stator vanes or fan blades. A parametric set of modes was generated at either the forward or aft driver set, and measured by the rotating rake in the opposite duct location. That is: the exhaust rake measured modes generated by the forward driver set; the inlet rake measured modes generated by the aft driver set. Fourteen or twenty-eight stator vanes were installed at various pitch angles and the rake mode measurements repeated. Separately, the rotor blades were installed at 3 different pitch angles. The nominal pitch angle for ANCF is 28° and that configuration was run at 3 different fan speeds. The fan pitch angle was changed by +/-10° and run at a single fan speed for those two angles.

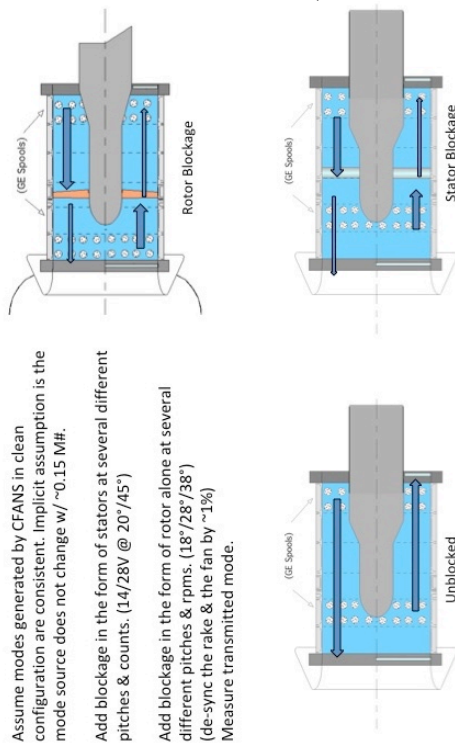
Duct mode propagation theory^{3,4} assumes a long duct as defined by the length to diameter ratio ($L/D > 1$) in order for the classic mode structure to develop into the predicted analytical forms. In reality, even a cut-off mode can be said to “propagate” from the source, albeit at a significant decay rate. Modes that are well below cut-on may decay at a rate of 80-100 dB per duct diameter, while a mode just below cut-on may decay at a rate of only 2-3 dB per diameter⁴. To investigate this effect, the ANCF/CFANS was tested with two duct lengths (Figure 8d) with the actuated driver row 1 diameter from the duct exit, or 1/4–diameter from the duct exit. The modes were measured at the inlet entrance plane. Corresponding farfield directivity data were acquired. The farfield array was kept at a constant distance from the duct inlet entrance plane. Modes and farfield directivity from the short and long duct configurations were noted to have significant differences. Duct modes in short-ducts have not decayed and are nearly equal in strength to the target mode. The total PWL in all modes, PWL in the generated mode, and the sum of the non-target mode were also compared.



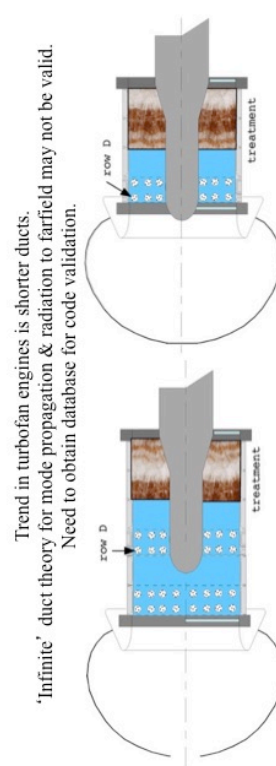
(a) Aft Duct Propagation (Eversman Radiation Code Variation)



(b) Inlet Distortion Experiment Configurations



(c) Transmission Loss / Blockage Experimental Configuration



(d) Effect of Short Duct on Modal Content / Farfield Directivity

Figure 8: Code Validation Configurations

D. Active Noise Control

As mentioned in the prior sections the ANCF was built to support the NASA Active Noise Control effort. ANC is the use of sound equal in frequency and spatial characteristics but 180° out of phase to the original resulting in destructive interference of the original acoustic field. An ANC system³⁵ requires 3 main components: detection microphones to measure the signal to be cancelled (or its residual), a control algorithm to determine the necessary signal, and actuators to generate the canceling acoustic signal. The NASA effort addressed the fan harmonics and utilized a modal approach. It implemented an increasing complexity approach by continuously introducing higher source content, actuator concepts, and more efficient control algorithms. The order of discussion that follows is not necessarily chronological, but grouped by concept.

The maiden ANC test was the GE ANC Flat Plate Actuator study³⁶ pictured in Figure 9a. The goal of this study was to assess the feasibility of using wall mounted secondary acoustic sources and sensors within a ducted fan for active noise cancellation of fan tones. The modal control system was based on a Single-Input, Single-Output RPM feed-forward controller using a modal control approach. The key results were that the (6,0) mode was completely eliminated at 2BPF (960 Hz). Global attenuation of tonal PWL was obtained using an actuator and sensor system totally contained within the duct. This was the first successful ANC test of a complex nature.

The next level in complexity was to effect control of the first two fan harmonics, with 2 radials at 2BPF, in the inlet, and to provide unidirectional control (that is no increase in noise in the exhaust direction). In addition, the active resonator concept was applied. HWAE developed active/passive resonator concept³⁷ whereby an active element in the actuator base extends the range of a Helmholtz resonator and slight broadband character of a resonator is maintained (see Figure 9b). The concept was successful as the three radials were attenuated (which actually required 6 control Mutli-Input, Multi-Output (MIMO) control channels to prevent an increase in the exhaust). The resonators were tuned at BPF and substantial attenuation is noted – the active portion has no effect. At 2BPF the passive has no effect and the active control reduces the farfield level.

The number of targeted radial modes was increased to four at $m=2$, 2xBPF in a task performed by GE using 4 rows of wall-mounted electromagnetic speakers as shown in Figure 9c. This radial mode density approaches that of a cut-on turbofan at BPF, or 2BPF at approach. Radial modes are more difficult to cancel since their axial wavelength can vary significantly. Indeed, this test ran into a radial distribution problem. The (2,1) mode was relatively low compared to others and was difficult to couple into and actually increased thereby limiting the net reduction. Later numerical simulations showed that this can be overcome by over-specifying the ANC control system by increasing the MIMO channels or increasing the duct length for the error sensor distribution (not really a potential option).

The emphasis on simultaneously developing actuator technology was continued as HWAE integrated piezoelectric drivers (Figure 9d) surrounding the stator vanes: 2-rows on the duct wall near the tip, and 2-rows on the hub, near the base of the stator. The additional utilization of the inner wall provided a more efficient coupling to the radial modes since there were now two radial direction boundary conditions specified. Multi-directional control in a more compact arrangement was successfully demonstrated.

Figure 9e pictures an attempt to simultaneously control multiple modes and harmonics in both the inlet and aft ducts. This was accomplished by combining the GE & HWAE systems from the earlier tests. Simultaneous multi-mode control of inlet/exhaust – 7 radials at $m=2$, 2BPF (4 inlet, 3 exhaust) – approaches the modal density of turbofans at 2BPF under most conditions. This combined control successful as the exhaust reduction was nearly the same as earlier separate control results. The inlet reduction was still limited by (2,1) radial increase but performed slightly better than separate control.

The preceding tests used the Adaptive-Quadrature (A-Q) control algorithm in single and multi-tone suppression systems, based on bandwidth capability, rapid convergence and processing simplicity

Taking advantage of the radial coupling of vane mounted actuators, attenuation of higher order radials was attempted in two separate entries^{38,39}. The development of the vane actuators was based on THUNDER actuator technology implemented by BBN. These are highly resonant to enable higher amplitudes to be generated – potentially at the level of full-scale turbofans, at least at approach. A schematic of the actuators and installation on the ANCF stator vanes is shown in Figure 9f. The results were the vane actuator ANC system reduced total 2BPF tone PWLs in the target modes in the inlet while at the same time exhaust power levels were reduced. A simplified control system with just two actuator arrays at different radial locations was demonstrated to simultaneously reduce tonal power in both inlet and exhaust. A benefit of vane actuators is that they act at the source of the disturbance. If both fan interaction and control sources are at the same location and are both dipole sources, then they should couple with the duct acoustics in the

same way. The baseline control strategy was successful, resulting in control of the seven radials in $m=2$ (four in the inlet, three in the exhaust). An important result from the baseline configuration was the simultaneous reduction in the inlet and exhaust when control was attempted in the inlet only. To say this is essentially an under-specified control system is a substantial simplification. The reason for this dual control is likely due to the close physical proximity of the anti-source (actuators) and the source (stator vanes). Other configurations in this test tended to confirm this result.

After the successful demonstration of ANC, it was recognized, and studies showed, that any loss of treatment required to install an active noise control system would result in penalties due to the loss of treatment that could be greater than that obtained from the ANC.

HAE/Rice developed an ANC system⁴⁰ that was coupled to a Grumman passive liner, which is pictured in Figure 9g. The ANC portion of the combined system was to “set-up” the two-targeted radial modes so that the passive liner was more effective at cancellation. The optimized active/passive liner achieved a greater reduction than either alone. Keeping the passive liner in the configuration maintained the broadband attenuation. Indeed, the combined system yielded greater attenuation than the sum of the active and passive acting separately – the hybrid generating a synergistic effect as intended.

While the aforementioned hybrid configuration demonstrated the efficacy of a combined/active system, the passive liner extent was reduced to incorporate sensors into the hardwall. An inlet duct section was used to investigate fully incorporating passive treatment into an ANC system that embedded the sensors, shown in Figure 9h. Comparisons were made of the ANC performance with baseline hard-wall (treated section taped over) to ANC performance with the treated section exposed along with a comparison was between using the error sensing microphones upstream of the exposed treatment and embedding the microphones in the treatment. The reduced levels achieved with sensors embedded in the liner were similar to those obtained with the sensors embedded in the upstream hardwall section, demonstrating that control can successfully achieved with sensors embedded in a liner. The ability to embed the sensors in the treatment increases the flexibility for the locating error sensors in ANC systems and avoids any noise reduction performance penalties associated with eliminating a very small portion of the passive treatment.

The component count required for successful ANC are specified by the physics of duct propagation. The full specification resulted in very high component counts (microphones and actuators) that are probably not feasible on an in-service turbofan. Therefore, attempts were made to reduce the component count.

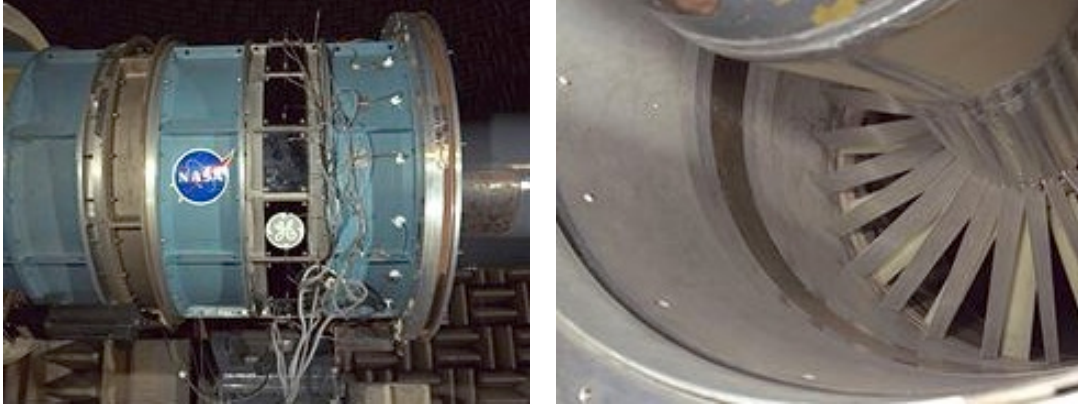
In the first attempt at simplification⁴¹, an axially distributed array was used instead of the complete circumferential array, to detect $m=2$ as shown in Figure 9i. This assumes that the target mode is dominant in the acoustic signature since an axial array does not allow for circumferential modal decomposition (a situation known from the character of ANCF). The minimum number of microphones required is still equal to the number of radials present (in this case, four in the inlet and three in exhaust for a total of seven). The results show that the reduction obtained is very modest, and there are even slight increases. It is important to recognize that the extraneous modes (non-target modes) generated by imperfections in the actuators and/or input signals result in modest reductions – though the concept might be valid.

The standard location for the ANC error sensors has typically been the duct walls. As seen earlier, this arrangement can have difficulty detecting radial modes. Alternative locations were investigated⁴² on the ANCF.

A boom was located outside the fan duct in the horizontal plane, approximately 10 feet from the centerline pictured in Figure 9j. The goal was to demonstrate the feasibility of reducing selected sectors in the farfield directivity that have the greatest impact on noise. This could be a more realistic application of the farfield error microphone technique, perhaps being mounted off an aircraft wing or fuselage. The boom array error sensing input weighting used two methods: a radial based filtering to attempt to control individual radials and an angle based method to control sectors in the farfield. The best results with the radial based filtering method were achieved by applying control weighting to the $m=2$ mode. Control weighting of other individual radials was not successful in providing reductions in the $m=2$ mode or for the corresponding individual radials. As was found with the steering array, the targeted mode was not necessarily the one reduced the most.

Turbofan engines typically have a pylon or bifurcation in the exhaust duct. The ANCF exhaust duct was modified by installing two radial surfaces 180° apart, in the vertical plane to simulate a bifurcation, which is pictured in Figure 9k. This surface can provide additional locations to mount error-sensing microphones. In addition, the radial extent of the pylon/bifurcation can provide radial information to the control system. Twenty microphones were distributed radially (five on each surface). A configuration using six microphones (three on two pylon faces) performed very well and met the goal of using only radially distributed microphones. It was suggested that more microphones are required in the radial distribution than the number of radials present.

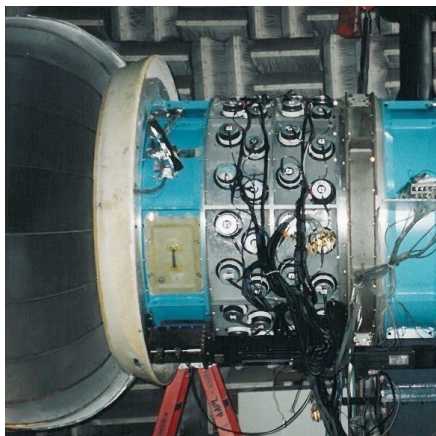
The ANCF demonstrated that tonal based ANC is possible, potentially significantly reducing multiple harmonics. It demonstrated that fully integrating the active system into a liner is necessary as well as close-coupling the actuators. It was generally recognized that the benefits of tonal control did not justify the added complexity – and attempts at reducing the complexity did not improve that cost/benefit ratio. The ANCF effort also demonstrated that the most critical component of the ANC system is the control algorithm. That was determined to be the basis of any research attempted in broadband ANC – which could potentially enable the cost/benefit ratio to become viable.



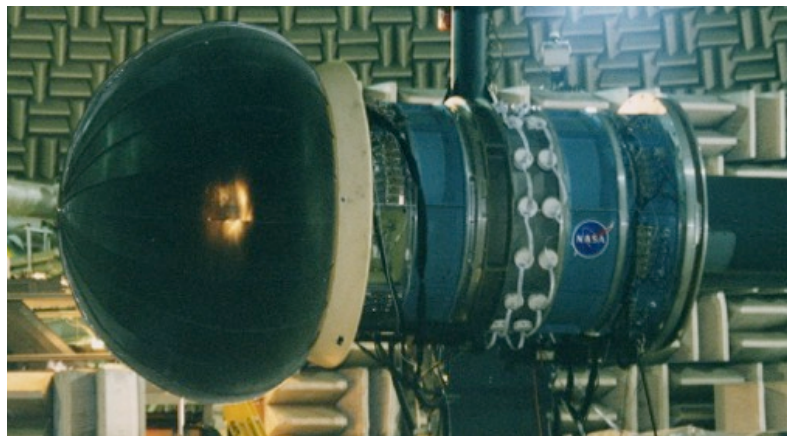
(a) GE ANCF Flat Plate Actuators



(b) HWAE Active Resonators

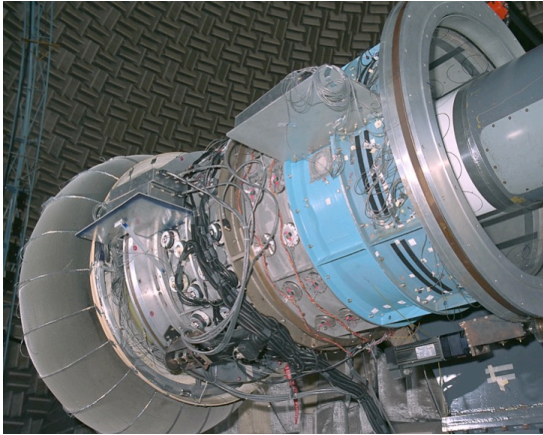


(c) GE Multiple Mode ANC

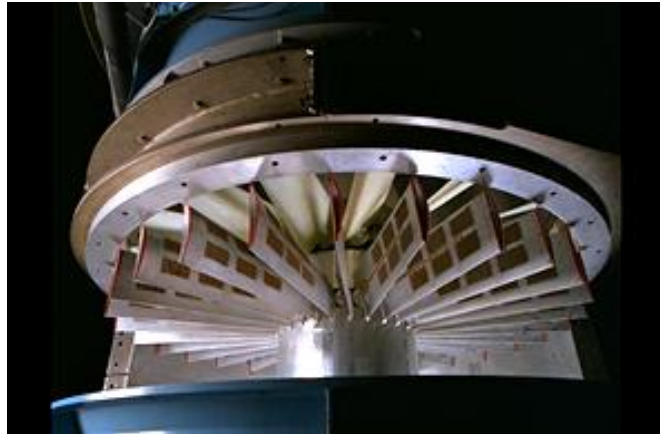


(d) HWAE Control Near Source

Figure 9: Active Noise Control Configurations



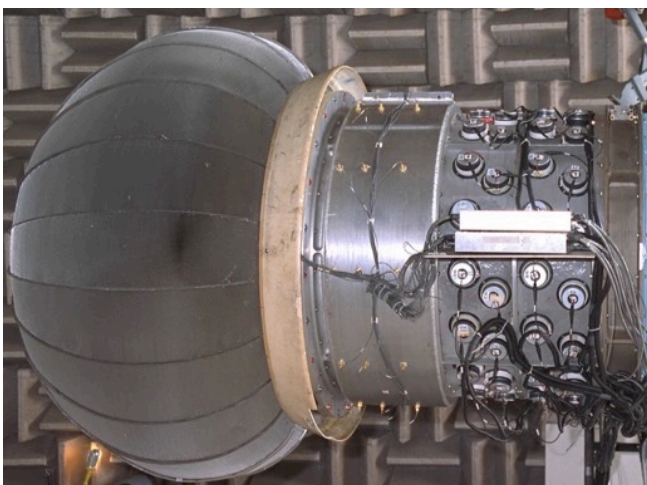
(e) GE/HWAE Combined ANC



(f) BBN Vane Actuators ANC



(g) Grumman/HAE/Rice Hybrid ANC



(h) Strategic Research Fund - Error Sensors Embedded in Liner

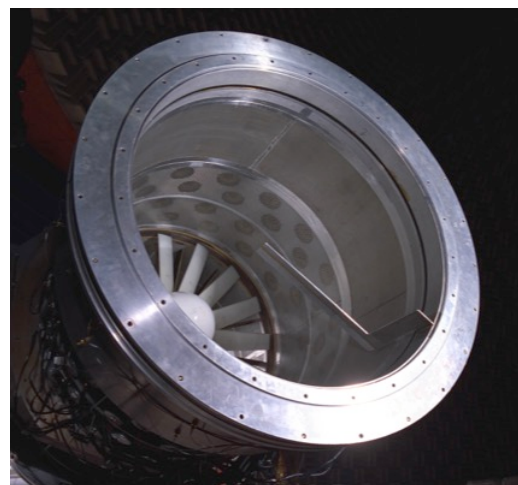
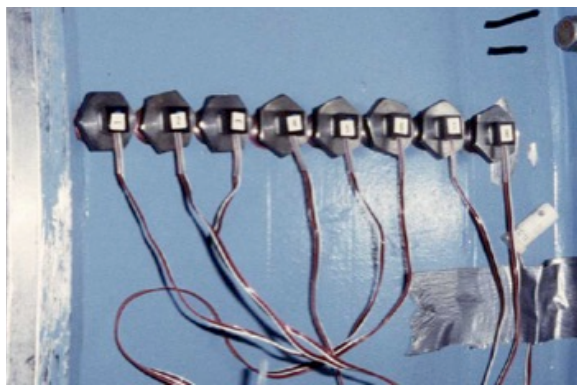
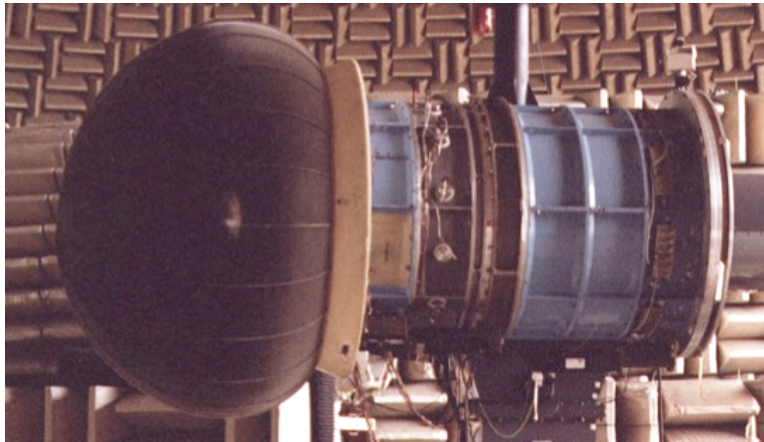
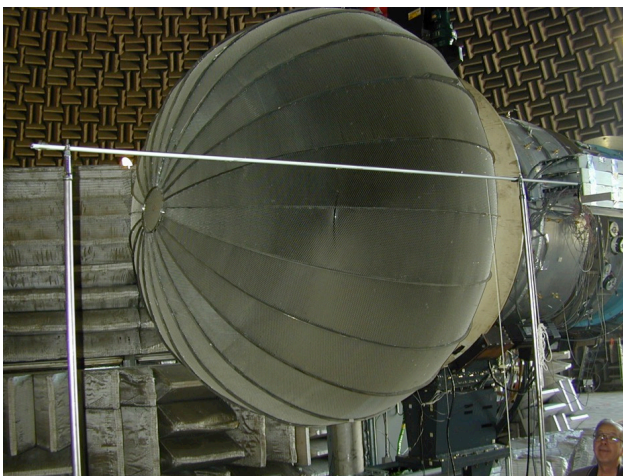


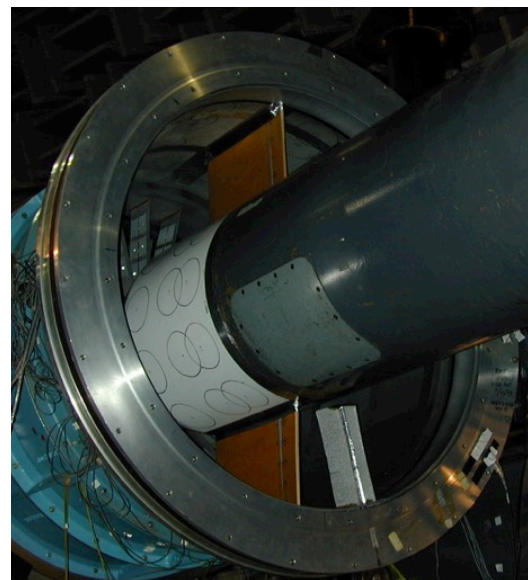
Figure 9: Active Noise Control Configurations



(i) VPI Linear Array



(j) HWAE Exterior Boom Array



(k) HWAE Pylon Error Sensor A

Figure 9: Active Noise Control Configurations

E. Unique Fan Noise Reduction Techniques

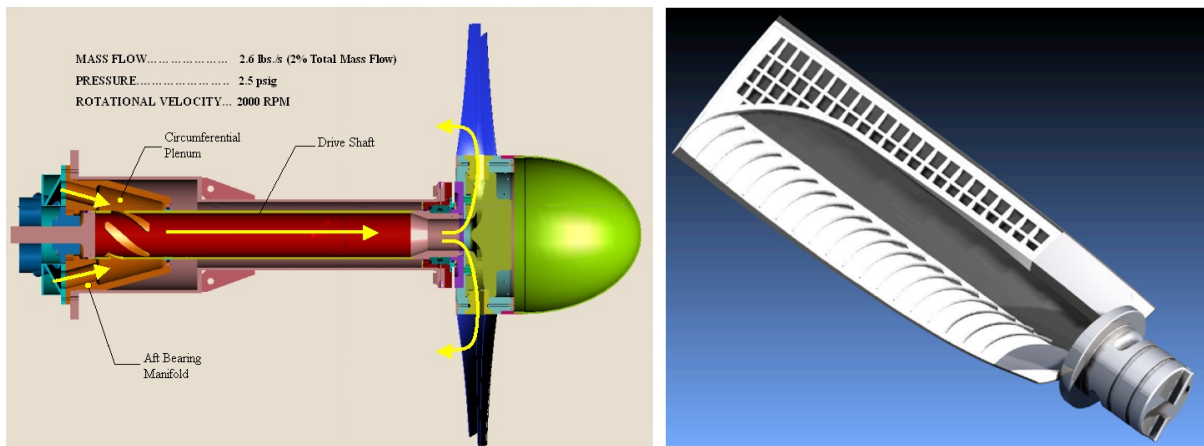
An experimental proof-of-concept test was conducted⁴³ to demonstrate reduction of rotor-stator interaction noise through Trailing Edge Rotor Blowing (TERB). The velocity deficit from the viscous wake of the rotor blades was reduced by injecting air into the wake through a trailing edge slot. Composite hollow rotor blades with internal flow passages were designed based on analytical codes modeling the internal flow. This hollow blade with interior guide vanes created flow channels through which externally supplied air flowed from the root of the blade to the trailing edge. The blade and air flow distribution system are shown on Figure 10a. The impact of the rotor wake-stator interaction on the acoustics was also predicted analytically. The ANCF/TERB rotor was designed using a modified version of the NASA developed compressor design program in conjunction with a three-dimensional viscous computational fluid dynamics (CFD) code for turbomachinery, RVC3D. A two-dimensional viscous CFD code, DVC2D⁴⁴, was used to a limited extent, for example, to simulate the flow field in the axisymmetric inlet upstream of the rotor, providing inlet boundary condition data for the rotor computational domain. The types of data acquired were: (i) two-component hotwire behind the rotor, (ii) unsteady stator vane surface pressures, (iii) acoustic duct modes, and (iv) farfield directivity. Reduction in the fan tone levels by filling the rotor viscous wake through trailing edge blowing was demonstrated to achieve substantial tone reduction using 1.6% to 1.8% of the fan mass flow rate. Indirect methods indicate that broadband reduction of rotor-stator interaction noise may result.

A fortuitous outcome of the TERB test was a rotor blade design that was more realistic than the original ventilation fan set. A set of blades based on the TERB planform, but with a sharp trailing edge, was used to update the baseline aero-acoustic data set^{10,13}. In addition, trailing edge inserts were made using rapid proto-type methods and materials to study passive mixing of the viscous wake (e.g. serrated or wavy – Figure 10b).

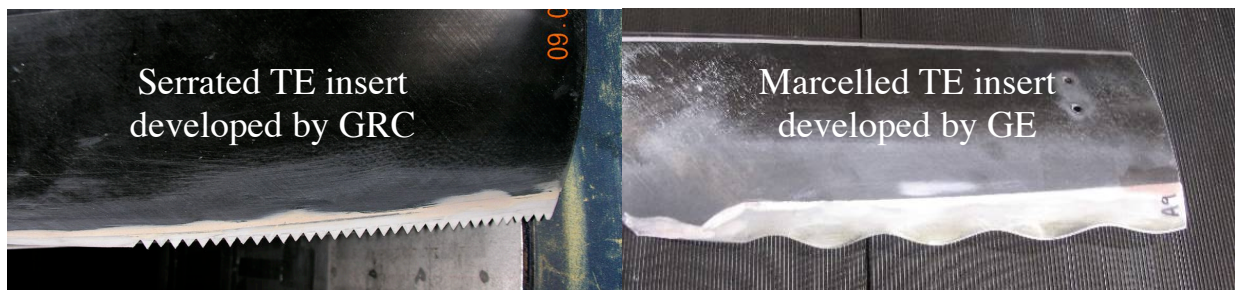
A foam-metal liner (FML) for attenuation of fan noise was developed for and tested on the ANCF⁴⁵ as shown in Figure 10c. A foam-metal liner was designed based on the absorption characteristics of the foam-metal determined using a normal incidence impedance tube and the known acoustic characteristics of a low-speed fan. The attenuation characteristics of the foam-metal-liner installed in the inlet matched the predicted absorption spectra reasonably well. Additional attenuation bandwidth, beyond that predicted from the impedance tube tests, occurred with the foam-metal-liner installed over-the-rotor (OTR), achieving broadband attenuation in both the inlet and aft farfield. This compared favorably to having single-degree of freedom liners installed in both the inlet and aft duct sections to achieve similar global attenuation. This suggests foam-metal liners installed over-the-rotor could provide the opportunity to eliminate the conventional liners, resulting in shorter ducts with reduced weight. A follow-on test of a FML/OTR on a production turbofan¹⁹ was performed and the impact on fan performance quantified based on these ANCF tests.

In order to better understand the physical effects of over-the-rotor acoustic treatments, a series of tests^{46,47} were performed at multiple TRLs, with various treatment concepts, of which tests on the ANCF were in the middle. Two locations were tested, (i) in a traditional inlet location, and (ii) in an OTR location. The goal was to measure the insertion loss of the four liners in the OTR configurations (Figure 10d) and compare to the same liners in the inlet, thereby providing some insight into the relative impact of the two physical mechanisms mentioned earlier. Each liner was evaluated in the ANCF in terms of acoustic reduction efficacy. In the OTR position, several of the liner designs were shown to have a reduction on the fan noise. The comparison of the reduction achieved in rotor-alone vs rotor-stator noise indicated that the attenuating mechanism is a combination of source modification plus a reduction in the propagating acoustic wave from the rotor-stator interaction, which is very notable in the forward arc.

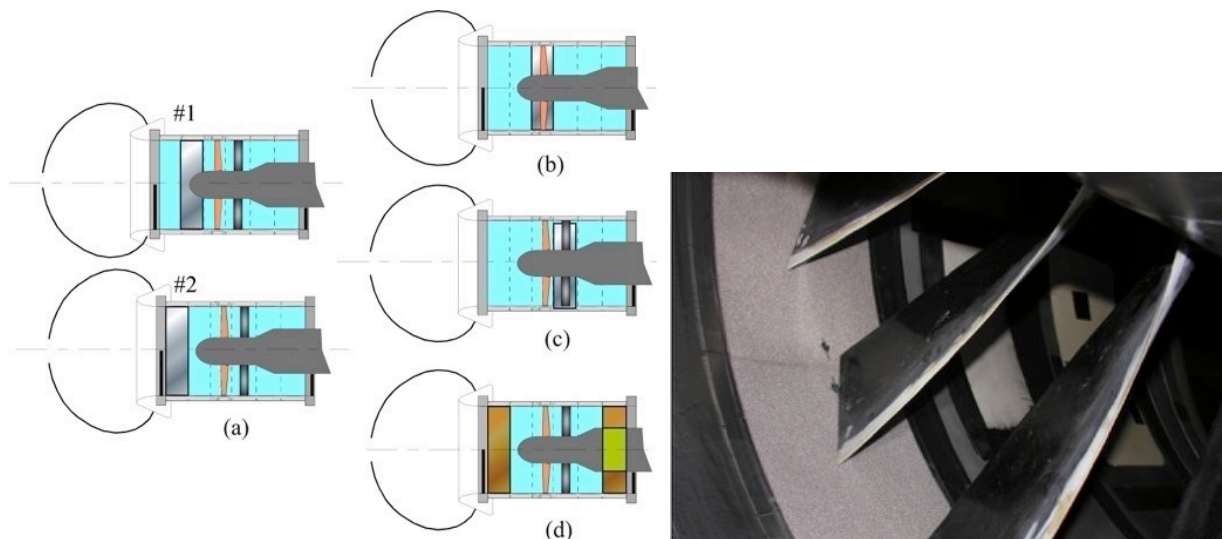
Extending the concept of passive treatment to locations other than the outer duct walls provides opportunities for additional attenuation. One potential location is the stator vane, where a portion of the stator vane surface is made porous to allow communication between pressure fluctuations at the vane surface and multiple, internal, resonant chambers. The internal chambers and porous surface are designed to an optimum impedance, such that maximum sound absorption is achieved. This impedance boundary condition also provides pressure release (relative to the rigid surface it replaces) at the surface of the stator vane. This concept has been termed “soft vane”⁴⁸ and is intended to reduce noise from rotor-stator interaction. Several soft vane configurations were tested on the ANCF, all utilizing the basic vane design. An exploded view of this concept is shown in Figure 10e. These were: (i) 2 rows of the interior partition beads filled with ceramic beads, (ii) same plus a fibermetal cover sheet over the porous area, (iii) the fibermetal cover sheet with only the interior partition, (iv) the fibermetal cover sheet with no partition, completely filled with ceramic beads, and (v) the fibermetal cover sheet with an empty vane. Configuration (ii) was the primary design and in fact achieved the best broadband attenuation relative levels to the original solid aluminum stator vanes. This broadband noise reduction was a very encouraging result, leading to a test on the high-speed ducted fan in the NASA 9x15 Wind Tunnel.



(a) Trailing Edge Rotor Blowing Configuration



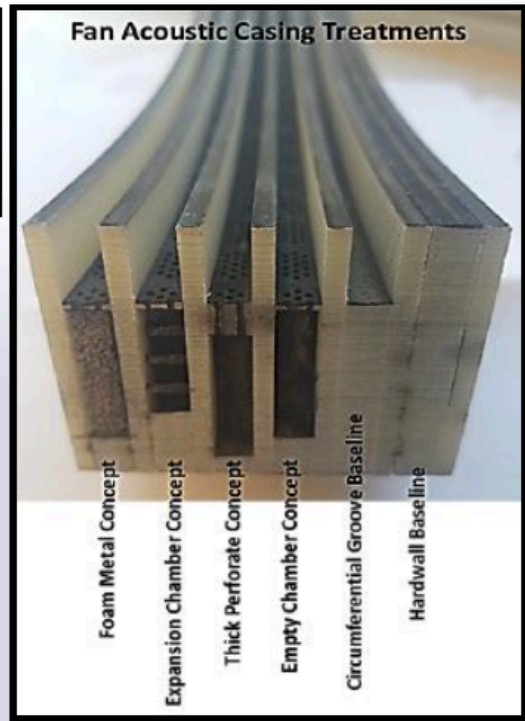
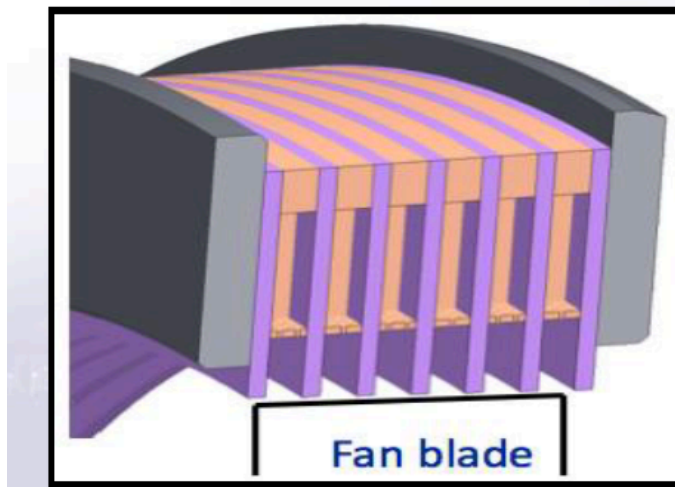
(b) Trailing Edge Inserts Adapted from TERB Blades



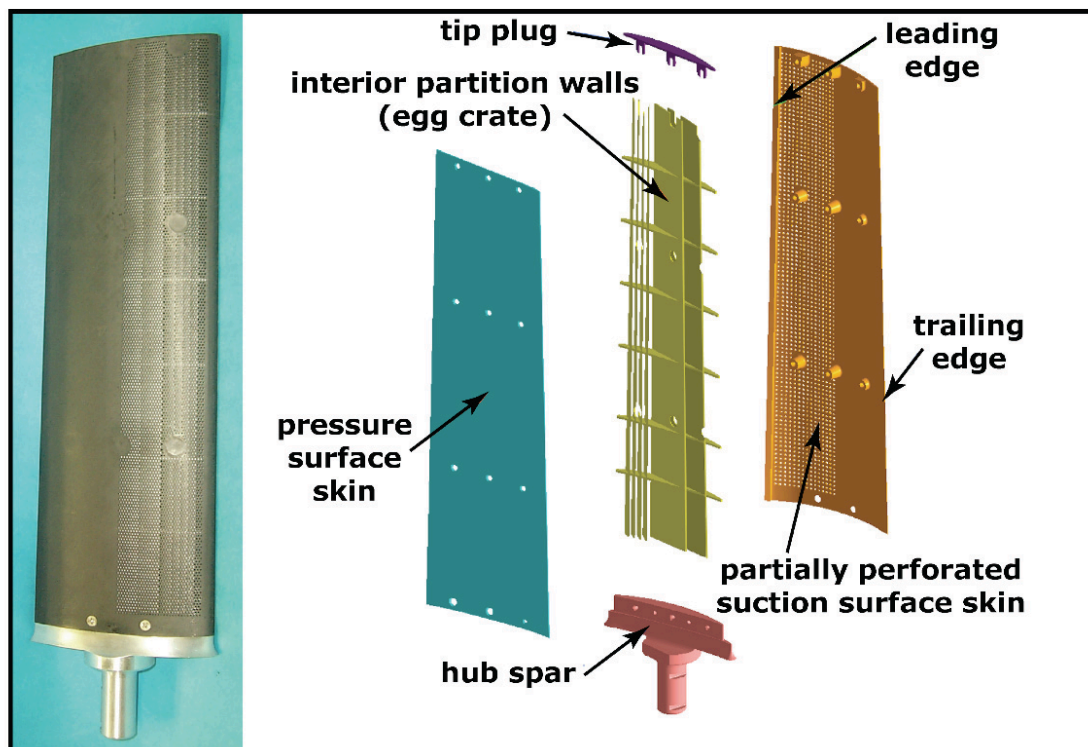
(c) Over-the-Rotor Foam-Metal-Liner Configurations

Figure 10: Novel Noise Reduction Configurations

CONFIGURATION ID	DESCRIPTION
I	Hardwall
II	Hardwall w/ Grooves
III	Empty Chamber w/ Thin Face Sheet
IV	Empty Chamber w/ Thick Face Sheet
V	Expansion Chamber w/ Thin Face Sheet
VI	Foam Metal w/ Thin Face Sheet



(d) Multiple Over-the-Rotor Liner Configurations



(e) Soft Vane Exploded Paper

Figure 10: Novel Noise Reduction Configurations

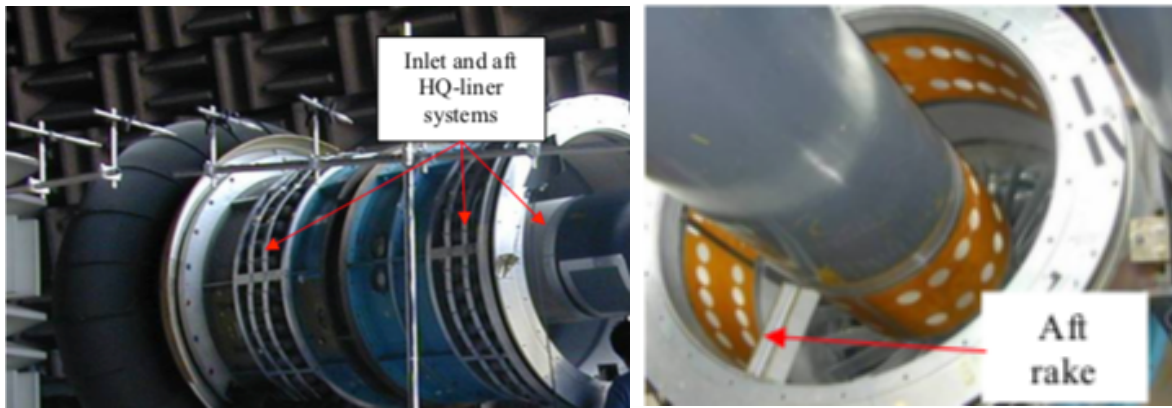
F. Novel Liner Development

As discussed earlier, the ANCF was designed to approximate the frequency range impacting the EPNL calculation. Any successful reduction over that range would benefit the public. The state-of-the art to attenuate that frequency range is passive liners. The ANCF was used to evaluate several advanced liner concepts.

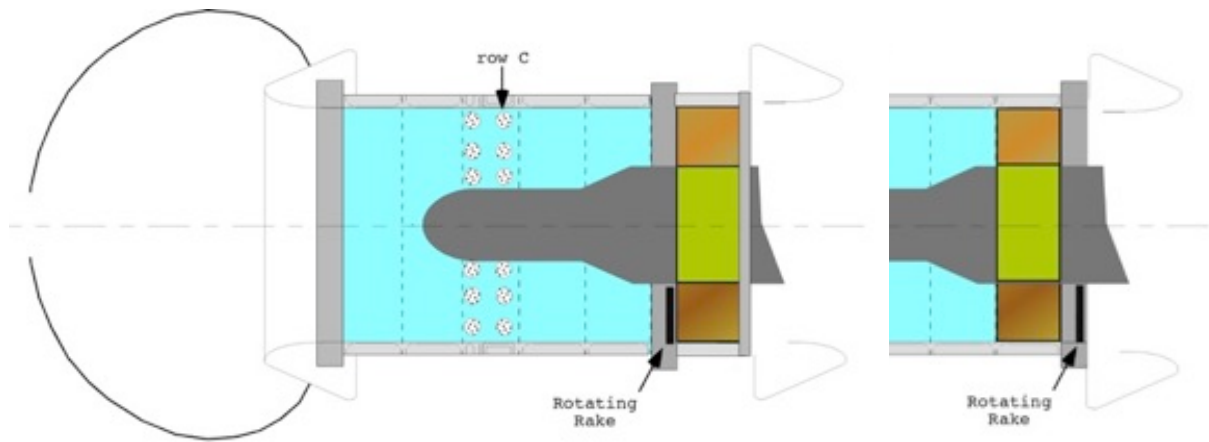
An experimental effort to investigate the performance of Herschel-Quincke (HQ) tubes combined with high resistance liners for the control of aft fan noise radiation was performed. In addition, testing of the HQ tubes with hard wall duct condition also performed. These are pictured in Figure 11a. The HQ tubes were specifically designed to attenuate the 2BPF tone and the broadband component around it. The liner was designed for optimum broadband performance between $2\frac{1}{2}$ to $5\frac{1}{2}$ BPF where the HQ contribution expected to be small. The HQ-liner system performed well: an encouraging contribution was from the HQ tubes, particularly at lower frequencies where the liner was not very effective. The HQ-liner test and results were used to justify the inclusion of HQ-tubes on the Honeywell TFE-731 technology maturation test program¹⁸.

Figure 11b shows the schematic of the ANCF configuration for the evaluation of insertion loss due to a liner. The liner used was a single-degree-of-freedom (SDOF) liner. The Rotating Rake was installed in one of two locations: upstream of the liner to measure the modal PWL at the entrance, and downstream of the liner to measure the modal PWL at the liner exit. Comparing the two measurements provides the liner insertion loss. This type of measurement provides a more detailed evaluation of the physics of the liner efficacy compared to just measuring the insertion loss in the farfield as it takes into account internal reflections and other acoustic effects. These rake locations were tested both with the liner exposed and taped over (to provide a hard-wall baseline). The effect of pylons on the liner efficacy was also investigated during this test. Two pylons were manufactured: (i) a large one that extended the full axial length of the liner, and (ii) a smaller one approximately 25% of the liner length. Both pylons are pictured in Figure 11c. Configurations tested were with both pylons mounted, or the large pylon only, for either the hardwall or liner. This investigation built on an earlier one that showed pylons reflect modes into the opposite rotation.

Two broadband liner designs⁴⁹ were produced that were predicted to provide increased attenuation over conventional tonal designs for the full range of frequencies and operating conditions considered. Both designs incorporated a septum to create two chambers. The first liner incorporated a septum with a constant depth (same depth in each chamber) to provide a constant impedance liner design. The second design incorporated a unique variable depth septum creating a variable impedance liner. The insertion loss for each liner was measured experimentally. The objective of the experimental portion of this effort was to validate the efficacy of the design process by comparing the experimentally measured insertion losses for each liner to those predicted⁵⁰. In order to provide a clean, annular duct for this experiment the ANCF was built up off of the stanchion/pylon assembly that normally supports the fan and duct sections that make up the nacelle. That is, the spool pieces were stacked up in a vertical orientation on the floor as shown in Figure 11d. This removed the ANCF center-body and support pylon from the arrangement, providing a constant area annular duct. Two configurations were tested in this setup: (i) with a constant 24" diameter cylindrical tube center-body and (ii) with a constant 36" diameter cylindrical tube center-body. These provided an equivalent annular duct hub-to-tip ratio of 0.5 and 0.75, respectively (inner diameter of the outer wall is 48"). The entire stack rested on the floor, and approximately 6" of foam material was placed in the bottom of the stack to minimize reflections from the floor. Only in-duct rotating rake measurements using the CFANS as a source were acquired in this configuration. Obviously, in this orientation, there was no flow. Rotating Rake data were acquired at the entrance and exit of the liner. This was the primary setup for all liner configurations. Selected liner configurations were also installed on the standard ANCF configuration. The fan was used as the primary source at the standard range of 1400-2000 rpm pictured in Figure 11e. Two stator counts were utilized, 0 (rotor alone) and 14 vanes at 0.5 chord spacing. The liner was installed in the aft converging section where the hub-to-tip ratio transitions from 0.375 to 0.5. Rotating Rake measurements upstream and downstream of the liner were acquired. Farfield directivity measurements were acquired. The CFANS was also used to generate broadband noise as described above (no flow) and farfield measurements were acquired. These tests were used to assess NASA's ability to design acoustic liners using construction with embedded mesh-cap technique (developed by Hexcel Inc.). Data from the ANCF were compared with predictions from aero-acoustic propagation codes to demonstrate the prediction capabilities, and to compare results from different types of liner configurations. Based on the success in the ANCF (as well as the NIT and GFIT at NASA LaRC), similar liners were designed for tests on the DART⁵¹. This test clearly demonstrated that the MDOF configuration could be fabricated for a very difficult inlet configuration (14" diameter; strong curvature). This was used to convince program official that this type of design could be built in a flightworthy product and flight tested on a Boeing 737 MAX Quiet Technology Demonstrator testbed²⁰.



(a) HQ-tube Installation and Design

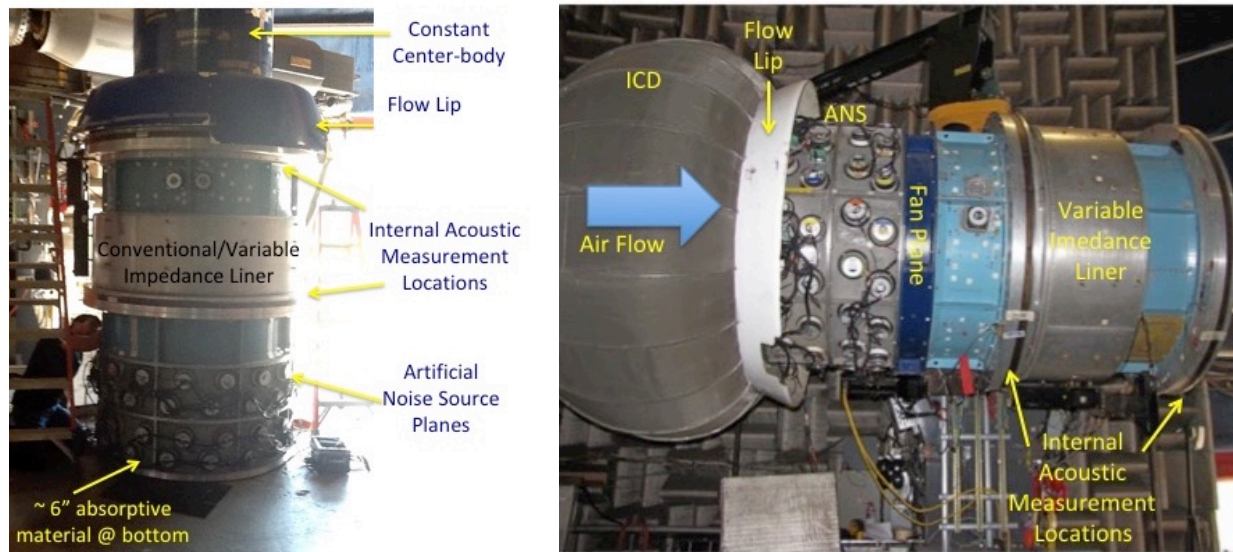


(b) Insertion Loss Measurement Configuration



(c) Effect of Pylon/Liner Interaction Configurations

Figure 11: Novel Liner Configurations



(d) Insertion Loss Measurement Configuration (e) Insertion Loss Measurements - Horizontal Configuration

Figure 11: Novel Liner Configurations

G. Measurement Technology Development

For reasons similar to those given for code verification (section III.C) the ANCF is well suited for development and improvement of aero-acoustic measurement technologies.

An expansion of the Rotating Rake measurement and analysis technique⁵² to include measurements over treated sections was validated using the ANCF. A rake with an extension measured the pressure profile over the passive liner (Figure 12a). Liners with differing impedances were evaluated by exposing them to several modes and frequencies generated by the CFANS. In addition to experimental validation on ANCF, the technique was verified by decomposing and analyzing radial pressure profiles generated numerically by the Eversman propagation code. Data from the ANCF fan with several different impedance conditions on the outer wall were acquired and reduced to determine the best fit. Using the impedance boundary conditions resulted in better mode measurement solutions. The methodology obtained basis functions based on wall impedance boundary conditions for flow conditions (i.e. constant duct area and Mach number) if the closed-form analytical solution existed. Analytical equations developed to estimate mode power are incorporated. For ducts with soft walls and mean flow, the radial basis functions must be numerically computed. The linear companion matrix method is used to obtain both the eigenvalues and the radial basis functions. In addition, a nonlinear least squares method is used to adjust the wall impedance to best fit the data in an attempt to use the rotating system as an in-duct wall impedance measurement tool.

Typically, a rake extending from the outer-wall to the duct centerline, has been inserted to measure duct modes at a single axial location. It has been known⁵³ that measurement at a single axial location will not be able to account for reflections in the duct; therefore, an experiment⁵⁴ utilizing an additional rake mounted on the same rotating ring as the original was conducted. This second rake was adjustable in the axial direction over the range of 2.5" to 10.5", in fixed, one-inch increments, and was mounted 180° from the original rake in the circumferential direction as seen in Figure 12b. Data were simultaneously acquired from both rakes to provide the two-point axial variation needed to compute the reflection. Reflections were created using two methods. The first method relies on the natural reflections due to an open-ended exit termination. The ring containing the dual rotating rake system was mounted at the exit of the ANCF stack-up. The single driver row (C) farthest from the exit termination was used to generate the modes (see Figure 12c). This configuration was run with the flow lip attached – this was assumed to minimize reflections; and with the flow lip removed, creating a sharp 90° flanged exit – this was assumed to create stronger reflections. A second configuration was used to generate artificial reflections. This was accomplished by locating the dual rake ring in the center of the stack-up. Driver row C was used to generate the “primary” wave and driver set B was used to generate the “reflected” wave. Each driver row was actuated independently and the dual rakes measured the modes. Then both

sets were activated simultaneously and the resulting superposition was measured. The concept is that the measured combination is the resulting superimposed mode and is equal to that measured independently and mathematically combined. The fixed rake mode PWLs were compared to the levels from the adjusted rake as a function of separation distance. The flow-lip on and flow-lip off cases were compared. The data showed that the mode PWL variation in axial distance is greater with the flow-lip removed, indicating a stronger reflection, due to constructive and destructive interference, as expected.

An available location for phased microphone arrays for determining engine inlet propagating mode distributions is the ICD (used on static engine tests). A proof-of-concept test⁵⁵ was performed on the ANCF, since the modal distribution of the fan tone harmonics were accurately measured by the Rotating Rake system. An array of 40 microphones were installed on the ANCF ICD; a close-up is shown in Figure 12d. An acoustic duct propagation code, CDUCT, was used to generate the steering vector predictions, required for classical phased array beam forming. The steering vectors consist of the CDUCT predicted complex acoustic pressure at the microphone locations for each propagating mode. The phase-accurate microphone data is then projected in the steering vector directions in order to determine the modal distribution. The dominant circumferential modes indicated by the ICD array matched those from the rotating rake.

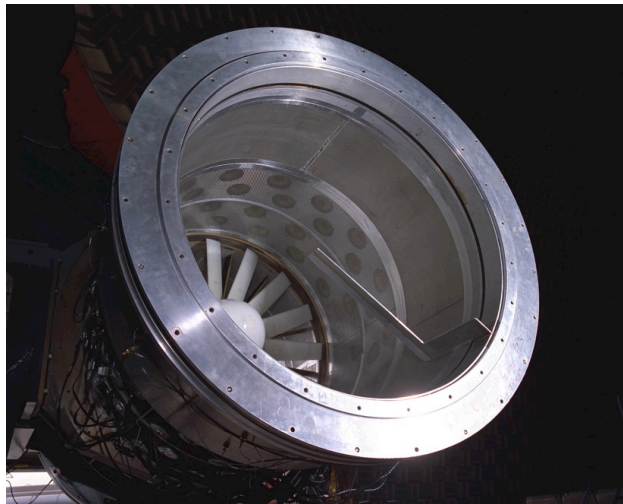
Another external technique that was investigated was a planar array in front of inlet⁵⁶, which may be more applicable for use in wind tunnels. This array is shown in front of the ANCF ICD in Figure 12e. The methodology utilized was to adapt the Generalized Inverse method and compute radiation patterns by approximating the Rayleigh Integral (Tyler-Sofrin) as a coherent sum over beam-form map points. A correction was applied by incorporating the Rayleigh integral with Kirchhoff factor. Included were the hardwall and pressure release modes.

An in-duct beam-forming technique for imaging rotating broadband fan sources was developed and evaluated⁵⁷. A phased array consisting of one or more rings of microphones was employed shown in Figure 12f. The data are mathematically resampled to a frame of reference rotating with the fan and subsequently used in a conventional beam-forming technique in the rotating frame. The steering vectors for the beam forming are derived from annular duct modes, so that effects of reflections from the duct walls are reduced. In contrast with other work, the steering vectors represent the effect of the unsteady pressure at the fan, rather than the Green's function. This improves the condition of the formulation and provides a connection to analytical studies. The test included a condition in which two of the fan blades were altered to create noise sources at known locations to provide a challenge. Comparisons of images obtained with a stationary rod installed in the inlet bottom dead center of the inlet using the VRM technique. The technique was evaluated by applying it to data from the ANCF rig with the Foam Metal Liner installed Over-the-Rotor. The evaluations suggested improvements to the technique could be made, which were subsequently implemented.

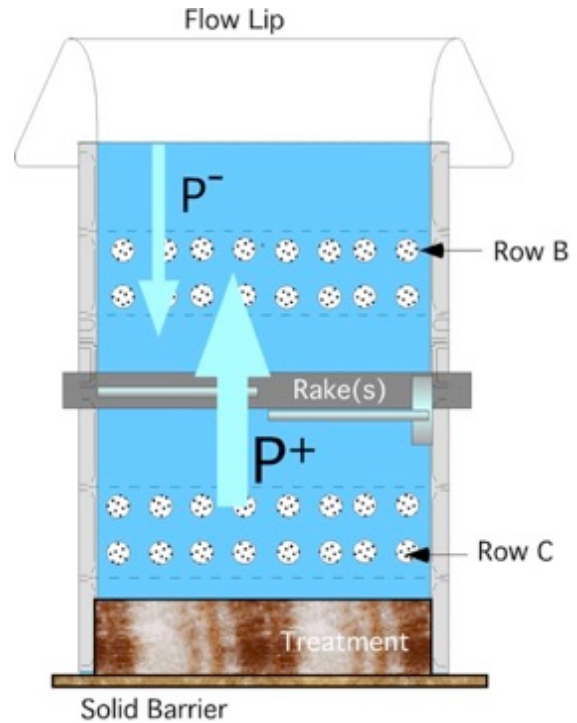
Farfield *inlet* fan noise can be measured under anechoic conditions in some model scale fan rig test facilities but farfield *aft* fan noise measurements are often not possible because the bypass flow is typically ducted away through a throttle into an exhaust stack. A beam-former based technique was developed⁵⁸ for processing measurements taken with an in-duct axial ('phased') array in the bypass duct of the ANCF (see Figure 12g) which, with certain modeling assumptions, enables the fan broadband noise level and directivity to be predicted in the farfield. Validation with a realistic fan noise source was partially achieved by using experimental data from the ANCF low-speed fan rig. The modal transfer functions are computed using a 'plug' flow exhaust model based upon a well-established Wiener-Hopf farfield technique but since the measured farfield data is located at three duct diameters from the exhaust, modal transfer functions are also computed at that distance and with a spreading jet model using a linearized Euler code. Both models yielded predictions that agree reasonably well with measured data but the latter is more accurate at small angles to the jet axis.

Typically, voltage values obtained from a hotwire must be corrected if the experimental temperature is different from the temperature at calibration. The experimental temperature is often not known exactly due to limitations in placement of a temperature measurement device. In addition, the temperature may vary in any of the dimensions that hotwire data is acquired. Generally, this is not a major cause for concern since (1) the temperature variation during the revolutions acquired is small; (2) the exact mean values are of less concern than relative or fluctuating values. Therefore, a single bulk experimental temperature is often used to correct all voltage measurements in a given run. However, using a single temperature across the entire revolution was unacceptable for the TERB application because of the significant temperature rise in the injected air. The compressor that supplied the injected air had a 30 to 40 °F temperature rise. In addition, the large temperature difference between the calibration (~70 °F) and the experiment (~30 to 40 °F) is probably greater than can be accurately adjusted by the standard temperature correction. Therefore, the two overheat method⁵⁹ was used to determine the true velocity and temperature across a passage. The hotwire

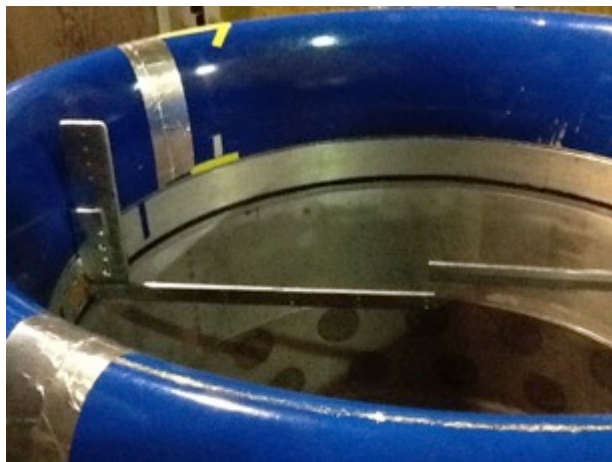
probe was calibrated, and data acquired behind the rotor, at two overheat ratios. The significant temperature rise in the wake changed the reduced velocity profile substantially when compared to the uncorrected, presumably inaccurate, profile obtained using a constant temperature across the passage profile. For the blowing case, it was expected that there was a temperature rise in the wake. The iterative method indicated that the peak rise is $\sim 4.5^\circ\text{F}$ near the centerline. In addition, the variation in the wake results in an iteratively converged velocity that has a significantly different characteristic than the velocity profile from either overheat ratio. The presumed actual velocity profile is overblown, a characteristic not indicated from the unadjusted profiles. In addition, both cases have nearly identical ($\sim 11.5^\circ\text{F}$) bulk temperature increases that are probably due to the systematic error in the temperature correction due to the large difference between the temperatures used for the calibration and the experiment.



(a) Modal Measurement Over Passive Liner



(c) Artificial Mode Reflection Generation



(b) Dual Rake Modal Measurement Configuration

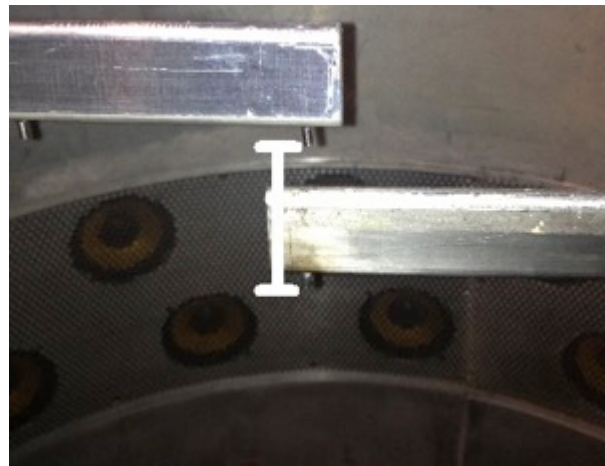


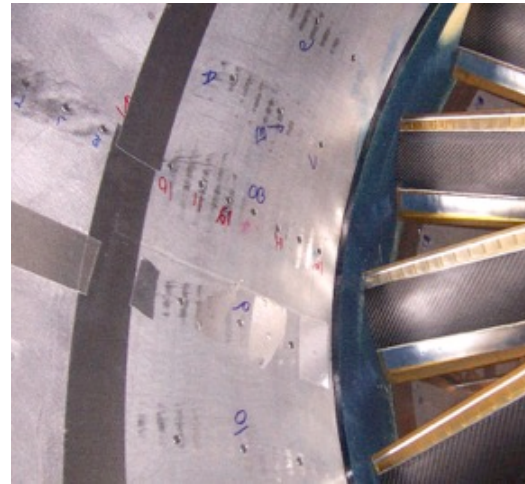
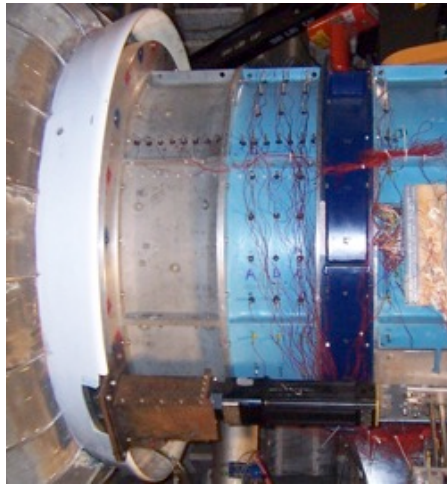
Figure 12: Measurement Technology Development Configurations



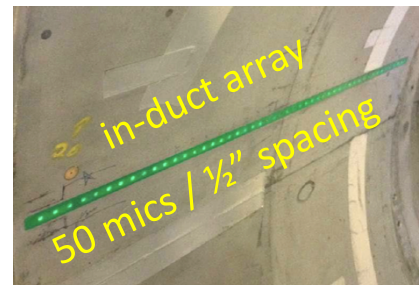
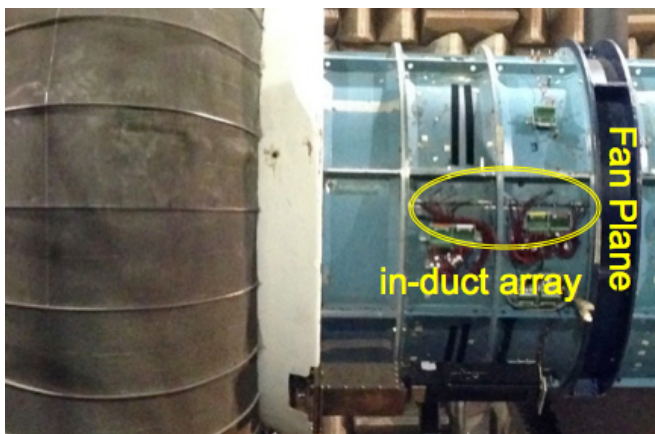
(d) Source Imaging Using an ICD Array



(e) External Flow-Through Array Configuration



(f) Source Localization Using an In-Duct Array



(g) Farfield Projection from In-Duct Array

Figure 12: Measurement Technology Development Configurations

IV. Summary

A. Proposed Replacement

Since 1995 the Advanced Noise Control Fan (ANCF) substantially contributed to the advancement of understanding of the physics of fan tone noise generation and the development of multiple fan noise reduction technologies. However, as the low speed/loading/pressure rise of ANCF was not fully representative of the physics of fan broadband noise generation, a replacement was considered necessary. In April 2010, consultation with industry/academia/government was held at the Acoustic Technical Working Group meeting at the Ohio Aerospace Institute to solicit opinions and high-level needs. This led to a request for resources to conduct a concept study for a replacement: “ANCF II”. The concept study team spent a year evaluating performance levels, infrastructure requirements, and multiple drive options. Industry comments were solicited, budgetary constraints noted, and results incorporated into a final recommendation. The ANCF II concept study results were presented to the project office on June 2011. The project office approved the further work and committed resources through the Preliminary Design Review that was held in September of 2012. The team recommended to the aero-acoustics community a design⁶⁰ for a 3000 HP electric motor, shaft driven fan in a 22-inch diameter duct that could be driven from the front or aft to enable clean farfield measurements in either arc. Unfortunately, the estimated costs were not within the budgetary scope and the effort was halted.

B. Collaboration

In addition to the highly prolific NASA studies accomplished, significant international collaboration transpired (Figure 13) using the ANCF on an explicit test, and/or its all-encompassing database of geometry and aero-acoustic data. Several students earned advanced degrees based on collaborations centered on the ANCF. A student from the University of Akron proposed and participated in custom modifications to the operating procedure to acquire transient data for his Master’s thesis⁶¹. Students from the Federal University of Brasilia developed a CAA code for their Master’s⁶² and Ph.D.⁶³ theses that used the 2008 geometry and data set for validation. At the University of São Paulo, a student based his Master’s Degree topic⁶⁴ on duct modal measurements from an internal array installed on the ANCF and comparisons to the Rotating Rake. A student from the University Southampton based a part of her Ph.D. thesis on a collaborative test with inter-stage liners⁶⁵. The University of Sherbrook⁶⁶ and ONERA utilized the available data/geometry package to validate their in-house CAA codes. Commercial codes from NUMECA (FINE™/Acoustics) and EXA (PowerFlow)⁶⁷ were partially validated using the data/geometry package. An interesting YouTube video⁶⁸ was created to demonstrate the results. There have been multiple Space Act Agreements, including three international (FUB, USP, and ISVR), focusing on collaborating using the ANCF. A simplified version of the ANCF was designed and manufactured, and is used for research at USP⁶⁹.

C. Relocation

In order to make room for a small turbofan engine (DART⁷⁰) the ANCF was relocated to the University of Notre Dame Turbo-machinery Research Lab (Figure 14). As a result of this change of venue the ANCF will be an outdoor test rig using ground-plane microphones and will be transported over a ¼ mile from the storage to the test site along the path. In spite of these significant differences, the farfield data comparison of the data acquired in the AAPL facility to the new University of Notre Dame (UND) outdoor location is remarkably similar. The use of ground microphones showed a simpler experimental setup can be useful in the acquisition of farfield acoustic data in an outdoor environment. For the most part, ground microphone data appeared to resemble pole microphone data, validating the usage of the former in outdoor experimentation. Furthermore, data acquired at UND decade apart from those acquired at NASA seemed as a positive indication of the healthy state of the fan. A paper⁷¹ detailing the initial commissioning test at UND’s facilities is published concurrently.

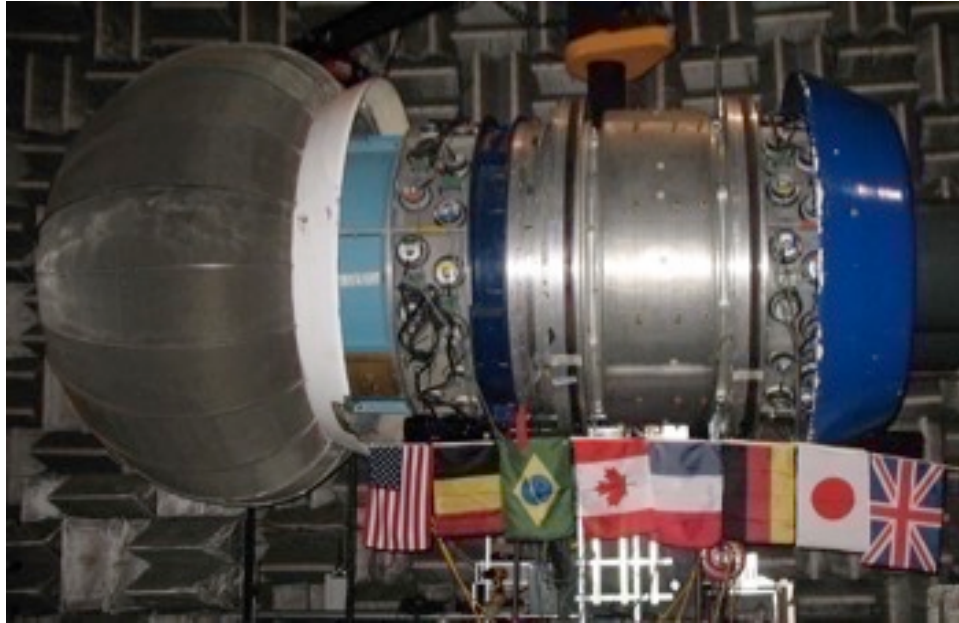


Figure 13: Flags of Many Nations Conducting Research on ANCF.

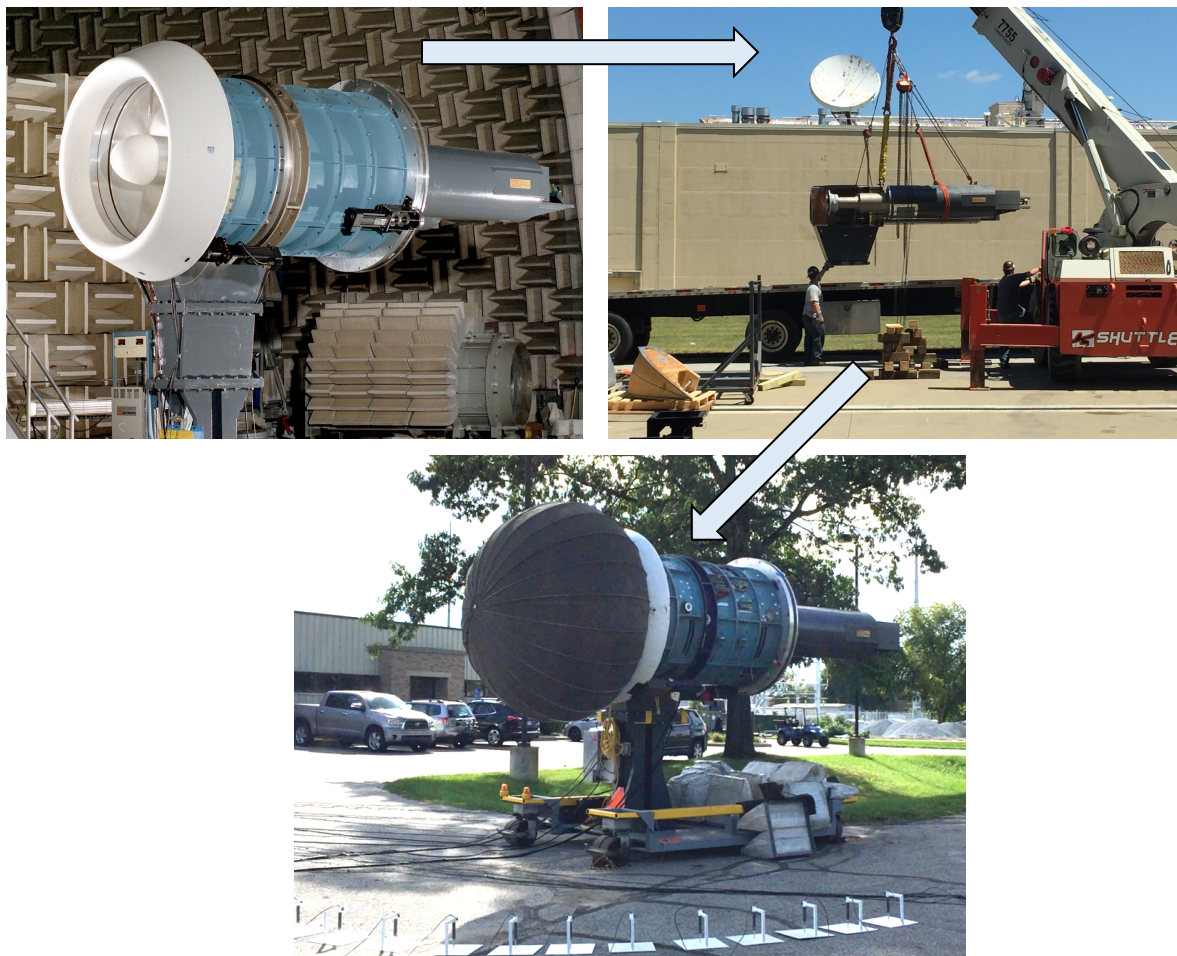


Figure 14: Relocation of ANCF.

V. Conclusion

The ANCF has contributed considerably to the various NASA ARMD research programs focused on reducing aircraft noise and mitigating its impact on the public. It is a complete aero-acoustic data/geometry set that is publicly available. The ANCF served as a wide-ranging enabler of cross-center, academic, industry, and international collaboration. It is a highly prolific test rig that is flexible, adaptable, that evolved to make wide-ranging contributions to the field of aeroacoustics for over 20 years and beyond including developing several technologies that were evaluated on production turbofans (static and flight test). Transferring the ANCF to the UND to jointly operate the test rig will maintain research its capability, and provide relevant STEM opportunities in the area of fan aeroacoustics. A more detailed version of this paper is presented in a NASA Special Publication⁷².

ACKNOWLEDGEMENTS

The author thanks Mr. Larry Heidelberg, who originally conceived of the Active Noise Control Fan, and significantly influenced him. Tony Shook, Julius Giriunas, and Kevin Konno contributed considerably to the design and installation of the ANCF. Technical support during the crucial early years was expertly provided by David Hauser, Michael Bronczek, Rick Herrlick and Ben Dastoli. Steve Wnuk provided professional engineering support during the early-to mid-operational years. Aero-Acoustic Propulsion Laboratory facility staff (Mark Jacko, Lenny Smith, Bruce Groene, Ed Mysliwiec, Joeseph McAllister, Joel Lauer, Mark Lasky, Devin Podboy, and Brian Rouse) and predecessor organizations continued the tradition of exceptional support. Current high-level managers in ARMD were operations engineers on ANCF (e.g. Ruben Del Rosario). Michael Jones and Douglas Nark, of the LaRC, exhibited the ideal of inter-center cooperation during numerous collaborations. Dr. Bruce Walker, who was also very influential on the author, was a prolific and significant contributing external researcher. Mr. Ray Loew is especially recognized in memory of his dedication and commitment.

REFERENCES

- ¹ Huff, D.L., "NASA Glenn's Contributions to Aircraft Engine Noise Research", NASA/TP—2013-2178185.
- ² <https://airandspace.si.edu/stories/editorial/nasa-leader-explains-why-failure-sometimes-option>
- ³ Hubbard, H. H., editor, Aero-acoustics of Flight Vehicles: Theory and Practice: Volume 1: Noise Sources, NASA Reference Publication 1258, Vol 1, WRDC Technical Report 90-3052.
- ⁴ Tyler J.M., and Sofrin T.G., "Axial Flow Compressor Noise Studies," SAE Transactions, Vol. 70, 1962, pp. 309-332.
- ⁵ Huff, D.L. "Noise Reduction Technologies for Turbofan Engines", NASA/TM-2007-214495.
- ⁶ Woodward, R.P., Hughes, C.E., Jeracki, R.J., and Miller, C.J, "Benefits of Swept and Leaned Stators for Fan Noise Reduction", NASA/TM-1998-208661.
- ⁷ Hubbard, H. H., editor, Aero-acoustics of Flight Vehicles: Theory and Practice: Volume 2: Noise Control, NASA Reference Publication 1258, Vol 2, WRDC Technical Report 90-3052.
- ⁸ Heidelberg, L.J., Hall, D.G., Bridges, J.E., and Nallasamy, N., "A Unique Ducted Fan Test Bed for Active Noise Control and Aero-acoustics Research", NASA TM-107213, also AIAA-96-1740.
- ⁹ Sutliff, D.L., Nallasamy, N., and Elliott, D.M., "Baseline Acoustic Levels of the NASA Active Noise Control Fan Rig", NASA TM-107214, also AIAA-96-107214.
- ¹⁰ McAllister, J., Loew, R.A., Lauer, J.T., and Sutliff, D.L., "The Advanced Noise Control Fan Baseline Measurements", NASA/TM-2009-215595, also AIAA-2009-0624.
- ¹¹ Cooper, B.A., "A Large Hemi-Anechoic Chamber Enclosure for Community-Compatible Aeroacoustic Testing of Aircraft Propulsion Systems", Journal of the Institute of Noise Control Engineering of the USA, Jan/Feb 1994.
- ¹² Sutliff, D.L., "Acoustic Characteristics of the Active Noise Control Fan Located in the Compact Farfield Arena", Technical Progress Report, Contract NAS3-00170, Task Order no. 17, Sest Inc.
- ¹³ Loew, R.A., Lauer, J.T., McAllister, J., and Sutliff, D.L., "The Advanced Noise Control Fan", NASA/TM-2006-214368, also AIAA-2006-3150.
- ¹⁴ Bozack, R.F., Jr., "Advanced Noise Control Fan Aerodynamic Performance", NASA/TM-2009-215807.
- ¹⁵ Homyak, L., Mcardle, J. G., and Heidelberg, L. J. "A Compact Inflow Control Device for Simulating Flight Fan Noise", AIAA 83-0680.
- ¹⁶ Sutliff, D.L. "Rotating Rake Turbofan Duct Mode Measurement System", NASA TM-2005-213828.
- ¹⁷ Sutliff, D.L., and B.E. Walker, B.E., "Artificial Noise Systems for Parametric Studies of Turbo-machinery Aero-acoustics", International Journal of Aero-acoustics January-March 2016 15: 103-130.
- ¹⁸ Weir, D., "Engine Validation of Noise and Emission Reduction Technology Phase I", NASA/CR-2008-21-13843A.

- ¹⁹ Sutliff, D.L., Jones, M.G., and Hartley, T.C., "High-Speed Turbofan Noise Reduction Using Foam-Metal Liner Over-the-Rotor", *Journal of Aircraft*, Vol. 50, No. 5 (2013), pp. 1491-1503.
- ²⁰ Norris, G., "Quiet Quest", *Aviation Week & Space Technology*, September 2018, pp24-25.
- ²¹ Sutliff, D.L., and B.E. Walker, B.E., "Two-Dimensional Air-Flow Tests of the Effect of ITA Flowliner Slot Modification by Grinding/Polishing on Edge Tone Generation Potential", NASA/CR-2004-213405.
- ²² Sutliff, D.L., Clifford A. Brown, C.A., Walker, B.E., "Hybrid Wing Body Shielding Studies using an Ultrasonic Configurable Fan Artificial Noise Source Generating Typical Turbofan Modes", AIAA 2014-0256.
- ²³ Sutliff, D.L., "Acoustic Characteristics of the Active Noise Control Fan Located in the Compact Arena", NAS3-00170-17, June 2002.
- ²⁴ Meyer, H.D., and Envia, E. "Aeroacoustic Analysis of Turbofan Noise Generation", NASA CR 4715, March 1996
- ²⁵ Sutliff, D. L.; Bridges, J., Envia, E., "Comparison of Predicted Low Speed Fan Rotor/Stator Interaction Modes to Measured", NASA-TM-107462, AIAA-97-1609.
- ²⁶ Sutliff, D. L.; Heidelberg, L. J., Envia, E., "Coupling of Low Speed Fan Stator Vane Unsteady Pressures to Duct Modes: Measured versus Predicted", NASA/TM-1999-209050, AIAA Paper 99-1864.
- ²⁷ Eversman, W., "Turbofan Acoustic Propagation and Radiation", NASA Technical Report, NAG3-2109, June 2001.
- ²⁸ Nallasamy, M., Sutliff, D.L., and Heidelberg, L.J., "Propagation of Spinning Acoustic Modes in Turbofan Exhaust Ducts", *AIAA Journal of Propulsion and Power*, Sep-Oct 2000.
- ²⁹ Heidelberg, L.J., Sutliff, D.L., and Nallasamy, M., "Azimuthal Directivity of Fan Tones Containing Multiple Modes", NASA TM-107464, AIAA 1997-1587.
- ³⁰ Koch, L., "An Experimental Study of Fan Inflow Distortion Tone Noise", 15th AIAA/CEAS Aero-acoustics Conference (30th AIAA Aero-acoustics Conference), 2009.
- ³¹ Koch, L., "Predicted and Measured Modal Sound Power Levels for a Fan Ingesting Distorted Inflow", AIAA-2010-3715, NASA TM-2010-216782.
- ³² Koch, L., "Validation of the Predicted Circumferential and Radial Mode Sound Power Levels in the Inlet and Exhaust Ducts of a Fan Ingesting Distorted Inflow", AIAA-2011-2808, NASA-TM-2012-217253.
- ³³ Koch, L., "Predicting the Inflow Distortion Tone Noise of the NASA Glenn Advanced Noise Control Fan with a Combined Quadrupole-Dipole Model", NASA-TM-2012-217673.
- ³⁴ Hixon, D.R., Envia, E., Dahl, M.D., and Sutliff, D.L. "Comparison of Computational Aero-acoustics Prediction of Acoustic Transmission Through a Three Dimensional Stator Geometry with Experiment", AIAA 2014-1405.
- ³⁵ Walker, B., "Sensitivity Issues in Active Control of Circular Duct Modes Using Axially-Spaced Actuator Arrays", *Proceedings of Active 99*, pp 91-102, The 1999 International Symposium on Active Control of Sound and Vibration, December 1999, Ft. Lauderdale, Florida, USA.
- ³⁶ Sutliff, D. L.; Hu, Z.; Pla, F. G.; Heidelberg, L. J., "Active Noise Control of Low Speed Fan Rotor-Stator Modes", NASA-TM-107458, AIAA Paper 97-1641.
- ³⁷ Walker, B.E., Hersh, A.S., Heidelberg, L.J., Sutliff, D L., Spencer, M.E., "Active Resonators for Control of Multiple Spinning Modes in an Axial Flow Fan Inlet", AIAA 99-1853.
- ³⁸ Sutliff, D.L., Curtis, A.R.D., Heidelberg, L.J., and Remington, P.J., "Performance of an Active Noise Control System for Fan Tones using Vane Actuators", AIAA 2000-1902.
- ³⁹ Sutliff, D.L., Remington, P.J., and Walker, B.E., "Active Control of Low-Speed Fan Tonal Noise Using Actuators Mounted in Stator Vanes: Part I Control System Design and Implementation", AIAA 2003-3193.
- ⁴⁰ Parente, C. A.; Arcas, N.; Walker, B. E.; Hersh, A. S.; Rice, E. J., "Hybrid Active/Passive Jet Engine Noise Suppression System", NASA/CR-1999-208875.
- ⁴¹ Smith, J.P., Burdisso, R.A., and Sutliff, D.L., and Heidelberg, L.J. "Active Control of Inlet Noise at the NASA Lewis Ducted Fan Facility", VPI-ENGR 97-444, Nov 1997.
- ⁴² Walker, B., Hersh, A., Celano, J., and Rice, E. "Active Control of Low-Speed Fan Tonal Noise Using Actuators Mounted in Stator Vanes Part 2: Novel Error Sensing Concepts", AIAA-2003-3191.
- ⁴³ Sutliff, D.L., Fite, E.B., E Envia, E., and Tweedt, D.L., "Low-Speed Fan Noise Reduction with Trailing Edge Blowing", *International Journal of Aero-acoustics*, 2002, Vol 1 No 3.
- ⁴⁴ Tweedt, D.L., Chima, R.V. "Rapid Numerical Simulation of Viscous Axisymmetric Flow Fields", AIAA-96-0449, also NASA TM-107103.
- ⁴⁵ Sutliff, D.L. and M.G. Jones, "Low-Speed Fan Noise Attenuation from a Foam-Metal Liner", *AIAA Journal of Aircraft*, July-Aug 2009.
- ⁴⁶ Gazella, M., Takakura, T., Daniel L. Sutliff, D.L., Bozak, R., and Tester, B.J. "Evaluating the Acoustic Benefits of Over-the-Rotor Acoustic Treatments Installed on the Advanced Noise Control Fan", AIAA 2017-3872.
- ⁴⁷ Bozak, R. F., and Dougherty, R. P., "Measurement of Noise Reduction from Acoustic Casing Treatments Installed Over a Subscale High Bypass Ratio Turbofan Rotor", AIAA Aviation Forum, 2018 (not yet published).
- ⁴⁸ Jones, M. G., Parrott, T. L., Sutliff, D. L., Hughes, C., "Assessment of Soft Vane and Metal Foam Engine Noise Reduction Concepts", AIAA-2009-3142.
- ⁴⁹ Nark, D.M., Jones, M.G., and Sutliff, D.L., "Improved Broadband Liner Optimization Applied to the Advanced Noise Control Fan", AIAA-2014-3103.
- ⁵⁰ Sutliff, D. L., Jones, M. G., and Nark, D. M., "In-Duct and Far-field Experimental Measurements from the ANCF for the Purpose of Improved Broadband Liner Optimization," AIAA-2014-3231.

-
- ⁵¹ Sutliff, D. L., Jones, M. G., and Nark, D. M., “Acoustic Directivity and Insertion Loss Measurements of Advanced Liners Installed the Inlet of the DGEN Aero-propulsion Research Turbofan”, NASA TM-2018
- ⁵² Sutliff, D.L. and Dahl, M.D., “Techniques for analyzing rotating rake mode measurements over passive treatment”, *International Journal of Aero-acoustics*, July 2016 15: pp 430-461.
- ⁵³ Cicon, D. E. and Sofrin, T. G., “Method for Extracting Forward Acoustic Wave Components from Rotating Microphone Measurements in the Inlets of Turbofan Engines,” NASA CR-195457, April 1995.
- ⁵⁴ Dahl, M.D. and Sutliff, D.L. “Analysis of Dual Rotating Rake Data from the NASA Glenn Advanced Noise Control Fan Duct with Artificial Sources”, AIAA 2014-3316.
- ⁵⁵ Lan, J., Premo, J., Sutliff, D.L., “Inlet Mode Measurements with an Inflow Control Device Microphone Array” AIAA 2002-2563.
- ⁵⁶ Dougherty, R.P., “Generalized Inverse Images of ANCF from Array 96 /Breaking News in Beamforming”, Acoustics Technical Working Group Meeting, NASA Langley, Hampton, VA, 23-25 October 2012.
- ⁵⁷ Dougherty, R.P., and Walker, B.E., “Virtual Rotating Microphone Imaging of Broadband Fan Noise”, AIAA-2009-3121.
- ⁵⁸ Tester, B.J., Özyörük, Y., Sutliff, D.L., and Bozak, R., “Validation of an in-duct to far-field beamformer method for predicting far-field fan broadband noise”, AIAA-2016-2894.
- ⁵⁹ *Hot-Wire Anemometry, Principles and Signal Analysis*, Section 7.4.2, Oxford University Press, 1995.
- ⁶⁰ Lucero, J., “Advanced Noise Control Fan II Test Rig and Trade Study Summary”, 2012, Oral/Visual Presentation, Report Number: E-661125.
- ⁶¹ Brown, C. A., “Analysis of Rotor-Stator Interaction Noise During a Speed Transient”, University of Akron Master’s Thesis, 2001.
- ⁶² Maldonado, Ana Luisa Pereira, “N Predição numérica do ruído tonal para o advanced noise control fan”, Universidade de Brasília, 2002.
- ⁶³ Pimenta, B. G., “Simulação numérica de ondas não-lineares em dinâmica dos gases e ruído de interação rotor-estator em turbofans aeronáuticos”, Ph.D. Thesis, Universidade de Brasília, 2016.
- ⁶⁴ Caldas, L. C., “Beamforming e análise modal em duto utilizando arranjo circular de microfones para caracterização de ruído banda-larga em motores aeronáuticos turbo-fan”, University of São Paulo, 2016.
- ⁶⁵ Maldonado, A.L.P., “On the prediction of the effect of interstage liners in turbofan engines”, *University of Southampton, Doctoral Thesis*, 2016.
- ⁶⁶ Sanjoséa, M., Daroukhb, M., de Laborderied, J., Sté Moreaue, S. and Mann, A. “Tonal noise prediction and validation on the ANCF rotor-stator configuration”, *Noise Control Engineering Journal* 63 (6), November-December 2015
- ⁶⁷ Mann, A., Perot, F., Suk K., Min, and Casalino, D. & Fares, E.. “Investigation of inflow condition effects on the ANCF aero-acoustics radiation using LBM”, 41st International Congress and Exposition on Noise Control Engineering 2012, INTER-NOISE 2012.
- ⁶⁸ CFD-Acoustic integrated simulation of the NASA Glenn Research Center's Advanced Noise Control Fan, <https://www.youtube.com/watch?v=pkraAk1YQwA>
- ⁶⁹ Caldas, L., Greco, P.C., Herold, G., and Baccalá, L.A., “In-duct Rotating Beamforming and Mode Detection of Fan Noise Sources”, AIAA 2016-3034.
- ⁷⁰ Sutliff, D.L., Brown, C.A., Bayon, B., and Sree, D., “Farfield Acoustic Characteristics of the DGEN380 Turbofan Engine as Measured in the NASA Glenn AeroAcoustic Propulsion Laboratory”, AIAA 2016-3006.
- ⁷¹ Figueroa-Ibrahim, K., Ross, M.H., & Morris, S., “Evaluation of Radiated Sound from the Advanced Noise Control Fan facility in an Outdoor Environment using Ground Microphones”, AIAA-2019-####.
- ⁷² Sutliff, D.L., “The Advanced Noise Control Fan: A 20 Year Retrospective of Contributions to Aeroacoustics Research”, NASA/SP-2019-643.